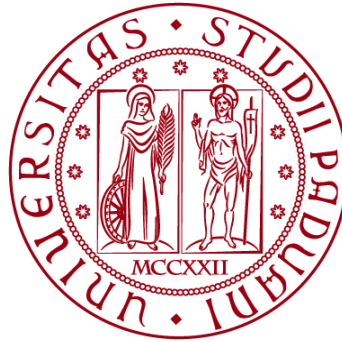


UNIVERSITÀ DEGLI STUDI DI PADOVA

DIPARTIMENTO DI BIOLOGIA

Corso di Laurea magistrale in Marine Biology



TESI DI LAUREA

"Ecology and ethology of a population of whale shark *Rhincodon typus* Smith, 1828 in Djibouti"

Relatore:

Prof.ssa Carlotta Mazzoldi

Dipartimento di Biologia

Correlatori:

Dr.ssa Francesca Romana Reinerò

Dr. Primo Micarelli

Centro Studi Squali-Istituto Scientifico

Laureanda: Lara Maule

ANNO ACCADEMICO 2022/2023

Abstract

Rhincodon typus (Smith, 1828) is the largest extant fish swimming in the warm tropical waters of the world. To protect and manage the conservation of this species, it is important to study its demography, ecology, and ethology. Whale sharks observed during the scientific expeditions organized by the Sharks Studies Center-Scientific Institute of Massa Marittima (GR) and carried out in Djibouti (east Africa) in 2017, 2020, and 2022 were photoidentified using the software I³S Classic. To date, 49 sharks are currently present in the database. Over the same 3 years period the average total length of the sharks measured through the laser-photogrammetry was 5.06 m. The frequencies of feeding behaviors were split as follows: in 2017, ram (or passive)-feeding (54.91%), suction feeding (31.08%), and active surface ram-feeding (14.01%); in 2020, suction feeding (56.67%), active surface ram-feeding (23.21%), and ram (or passive)-feeding (20.12%); in January 2022, ram (or passive)-feeding (44.56%), suction feeding (35.56%) and active surface ram-feeding (19.88%); and in November 2022, suction feeding (49.46%), ram (or passive) feeding (25.91%), and active surface ram-feeding (24.63%). All environmental factors were significantly correlated among them in influencing the feeding behaviors of whale sharks. Active surface ram-feeding was generally performed when there was a higher chlorophyll concentration in the water, higher light levels, no rainfall, lower temperatures of the water, and during La Niña ENSO (El Niño Southern Oscillations) events. Suction feeding was performed when the chlorophyll concentration was from medium to high, light levels were high, there was no rainfall, lower temperatures of the water, and during La Niña ENSO events. Ram (or passive) feeding was performed mainly when environmental factors included low chlorophyll concentration's levels, lower light levels, low rainfall, higher temperatures of the water, and during El Niño ENSO events. In conclusion, the ENSO phenomenon was not the major factor influencing the interannual sightings of whale sharks in the Djibouti area.

Keywords: whale shark, feeding behaviors, environmental factors, El Niño Southern Oscillation, interannual sightings.

Table of content

Abstract	2
1. Introduction	5
<i>1.1 Rhincodon typus</i>	<i>5</i>
1.1.1 Size, growth rate, and morphology.....	6
1.1.2 Skeleton	7
1.1.3 Teeth and Mouth.....	8
1.1.4 Skin.....	9
1.1.5 Muscles.....	10
1.1.6 Locomotion and buoyancy	10
1.1.7 Respiratory system	10
1.1.8 Reproduction	11
1.1.9 Nervous system	12
1.1.10 Digestive system.....	12
1.1.11 Circulatory system.....	13
1.1.12 Sensory system	13
1.1.12.1 Hearing system	14
1.1.12.2 Chemoreception.....	15
Olfactory system.....	15
Taste system	16
1.1.12.3 Vision system	16
1.1.12.4 Electroreception.....	17
1.1.12.5 Mechanoreception	18
1.2 Diet	18
1.3 Feeding behaviors.....	20
1.4 Movements	22
1.4.1 Horizontal Movements	22
1.4.2 Vertical movements.....	23
1.5 Threats	23
1.6 Conservation strategies.....	24
1.7 Ecotourism.....	24
2. Material and Methods	26
2.1 Sampling areas.....	26
Djibouti.....	26
2.2 Methods	27
Data Collection.....	27
2.3 Photoidentification	28
I ³ S Classic photoidentification software.....	28
2.4 Laser-photogrammetric survey.....	33
2.5 BORIS	36
2.6 Collection of Environmental data.....	38
2.7 Statistical analysis	39
3. Results.....	44

3.1 Photoidentification	44
3.2 Laser-photogrammetry	44
3.3 Feeding Behaviors.....	45
3.4 Influence of environmental factors on feeding behaviors and on interannual sightings of whale sharks in Djibouti	46
4. Discussion.....	55
4.1 Photoidentification	55
4.2 Laser-photogrammetry	56
4.3 Influence of environmental factors on feeding behaviors and related annually ethograms	57
4.4 Influence of ENSO events on the interannual sightings of whale sharks in Djibouti....	65
5. Conclusions	67
6. Appendix	69
7. References	70

1. Introduction

1.1 *Rhincodon typus*

Rhincodon typus Smith, 1828 was first described and named by Andrew Smith in 1828 in South Africa (Figure 1). Many common names were given to this species, both for the large range of distribution in the tropics and for the characteristic skin pigmentation. The whale shark's Japanese name is *jinbei zame*, the “patterned pyjama shark”, and in the Kenyan Swahili it is called *papa shillingi*, the “shark covered with coins” (Dove et al., 2021)



Figure 1-*Rhincodon typus* (Smith, 1828)

Source: Photo by Lara Maule, Djibouti 2022

R. typus belongs to the following taxonomic categories:

Kingdom: Animalia

Phylum: Chordata

Subphylum: Gnathostomata

Class: Chondrichthyes

Subclass: Elasmobranch

Order: Orectolobiformes

Family: Rhincodontidae

Genus: *Rhincodon*

1.1.1 Size, growth rate, and morphology

The whale shark is the world's largest extant fish species and perhaps the largest fish ever to have existed (Dove et al., 2021). In fact, the largest reliable record of a whale shark is 21m in total length (TL) (Chen et al., 2002) and several other records are also around 18m in TL (McClain et al., 2015). It is interesting to point out that the closest relative to whale sharks, the tawny nurse shark *Nebrius ferrugineus* (Lesson, 1831), is around 4m in maximum size (Pillans, 2003), which is a lot smaller even compared to the average size of whale sharks. Also, between other sharks not belonging to the order Orectolobiformes, only the basking shark *Cetorhinus maximus* (Gunnerus, 1785) (Figure 2) approaches the whale shark with 12m in TL despite it is not closely related (McClain et al., 2015). Most adult whale sharks are between 9 and 13m in TL and they can weigh around 15-18 tons with a life span estimated to be between 80 and 100 years (Dove et al., 2021). The whale shark has a slow growth rate of about 5.6 cm per year ($\pm 47.3cm$) (Rohner, et al., 2015): individuals kept in aquariums showed that new-borns grow faster than adult individuals and growth rate is faster in females than in males (Rowat & Brooks, 2012).

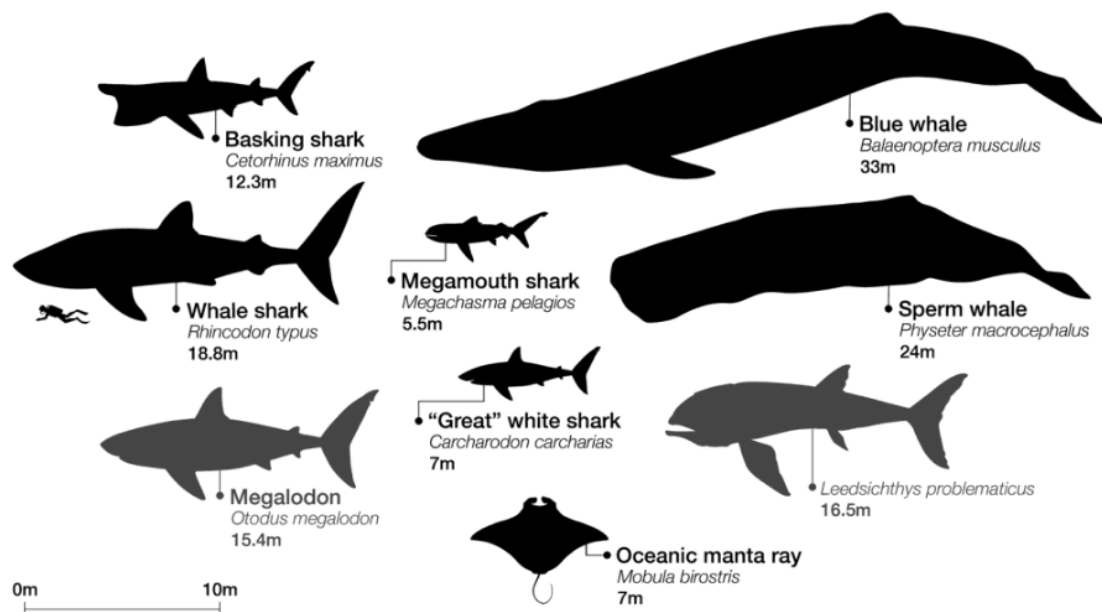


Figure 2-Comparative body size among marine vertebrates.

Source: Jen Richards Art, Dove & Pierce, 2021

R. typus is characterized by a broad, flattened head, a very large and nearly terminal mouth, very large gill slits, three prominent longitudinal ridges on its upper flanks (Compagno, 1984). The first dorsal fin is large, followed by a smaller second dorsal fin, a large semi-lunate caudal fin with the upper lobe larger than the lower lobe, two large pectoral fins, two smaller anal fins and pelvic fins (Norman, 2005). This species presents a unique pattern of light spots and stripes on a dark background with the ventral part light in color (Compagno, 1984). The pattern of spots that goes from the last gill slit to the end of the pectoral fin is a critical area for the photoidentification of individuals through the program *I³S Classic* (Interactive Individual Identification System). The program can compare and identify singular animals, facilitating the creation of databases to carry demographic research and more (Marshall & Pierce, 2012).

1.1.2 Skeleton

The endoskeleton of all elasmobranch species is made of a flexible and lightweight cartilage which can become hard and stiff if the calcium deposit increases, and this can happen specifically in the jaw, cranium, and vertebrae (Figure 3) (Kardong & Kennet, 2002).

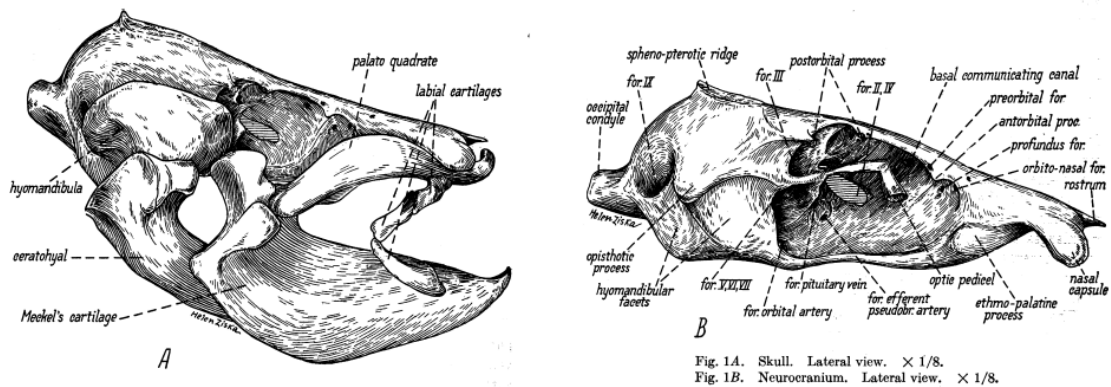


Figure 3- Anatomical representation of the cranium of *R. typus*

Source: Denison, 1937

1.1.3 Teeth and Mouth

Whale sharks have a very specialized mouth located in the front area of the head; it opens on the pharynx which on each side has five upper and five lower filtering pads which are modified gill rakers (Figure 4). They form a mesh supported by primary and secondary vanes and the whole pharyngeal basket can expand and contract because it is joined by flexible connective tissue (Motta et al., 2010). When feeding, the water rich of plankton enter the funnel shaped mouth and passes through the filtering pads; it then passes between the primary and secondary vanes of the gill rakers and then flows over the gill tissue to exit through the gill slits (Rohner & Prebble, 2021).

The jaws of *R. typus* have ribbon-like dental plates formed by many minute teeth. Each tooth is fixed, recurved backwards and acutely pointed (Figure 5). The number of teeth decreases towards the end of the jaw, and they are disposed in regularly transverse rows (Bean, 1907). Being the whale shark essentially a planktivore and a filter feeding animal, its teeth have little or no role in its feeding mechanism (Rowat & Brooks, 2012).



Figure 4 - Mouth of *R. typus* with visible filtering pads.

Source: Warren Baverstock, wetpixel.com

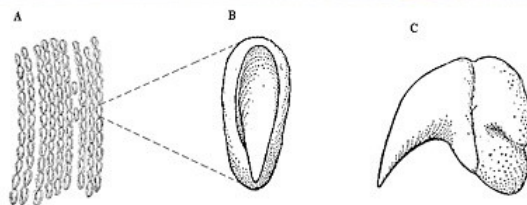


Figure 5 - *R. typus* dentition. A. Portion of the upper dentary band. B. top and C. lateral view of a single upper tooth.

Source: top, Cathleen Bester; bottom, Biegelow & Schroeder 1948.

<https://www.floridamuseum.ufl.edu/discover-fish/species-profiles/rhincodon-typus/>

1.1.4 Skin

R. typus has a unique skin pigmentation composed of light spots and stripes over a dark background color (Figure 6a). Although the evolutionary advantage of this pattern has not been investigated thoroughly yet, multiple theories, that may be all valid, have been reported:

1. the dorsal surface is useful to camouflage with the surrounding waters acting as a disruptive coloration, and the lighter ventral coloration has a countershading effect (Becerril-García et al., 2021).
2. the pigmentation may provide protection against the ultraviolet radiation to which this species is exposed by staying most of the time in surface waters (Becerril-García et al., 2021).
3. this species is known to form aggregations in feeding areas, and the pattern (which is different for each individual) may be useful for individual recognition between conspecifics (Martin, 2007).

The skin is covered by dermal denticles that have a hydrodynamic shape to reduce drag and noise production. In *R. typus* these denticles have three longitudinal ridges: the central one deeper forming a keel and the lateral with deep furrows on either side (Figure 6b) (Rowat & Brooks, 2012).



Figure 6a - Skin pigmentation of *R. typus*

Source: photo by Lara Maule, Djibouti 2022.

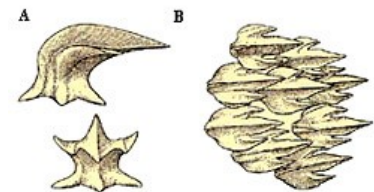
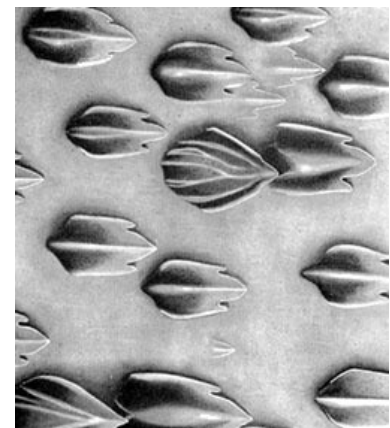


Figure 6b - Dermal denticles of *R. typus*. A. lateral and apical views of dermal denticles. B. dermal denticles.

Source: Garrick, Bigelow & Schroeder 1948.

<https://www.floridamuseum.ufl.edu/discover-fish/species-profiles/rhincodon-typus/>

1.1.5 Muscles

In sharks, two different muscle groups can be observed: just below the skin, a narrow band of red fibers lies on top of a thicker band of white muscle. The different coloration reflects the composition of the two groups: the red muscle is aerobic, highly vascularized and made for slow and continuous swimming. The white muscle is anaerobic and made for brief burst and fast swimming (Shadwick & Goldbogen, 2012).

1.1.6 Locomotion and buoyancy

Sharks are cartilaginous fish and they do not possess a swim bladder like bony fishes, instead they present a large liver containing squalene, an oily substance which guarantees a neutral buoyancy (Baldrige, 1970). Sharks, whale shark included, have retained negative buoyancy (they are heavier than sea water), possibly to save energy when descending into depths. Moreover, the angle the whale sharks keep during descents allows exceptional glide performance, which may be facilitated by the dorso-ventral flattening shape of their bodies (Gleiss et al., 2011).

1.1.7 Respiratory system

In all shark species, gills are positioned on the sides of the body, and they are the major structures involved in respiration (Hamlett, 1999). Their function is to absorb the oxygen



Figure 7 - Gills slits of *R. typus*

Source: Warren Baverstock, wetpixel.com

specialized gill rakers which are used to capture food particles. In fact, being filter-feeding animals, they present gill rakers very developed, long, and thin (Rohner & Prebble, 2021).

dissolved in the water and to release carbon dioxide. Each gill is composed of arches reinforced with skeletal elements, which sustain primary and secondary lamellae which are highly vascularized respiratory surfaces used for gas exchanges (Sherwood et al., 2012).

R. typus presents 5 pairs of large gill slits (Figure 7) and highly

1.1.8 Reproduction

Whale sharks are ovoviviparous animals: the embryos hatch from the egg cases inside the uterus of the mother and feed on the yolk until they are born, ready to swim and independent (Pierce et al., 2021).

The reproductive mechanism of whale sharks was unclear until 1995, when a pregnant female was caught in Taiwan and was studied. She was carrying roughly 300 embryos at different stages of development: some egg cases with the embryo still inside, some embryos had hatched from the eggs and were nearly ready for birth (Pierce et al., 2021).

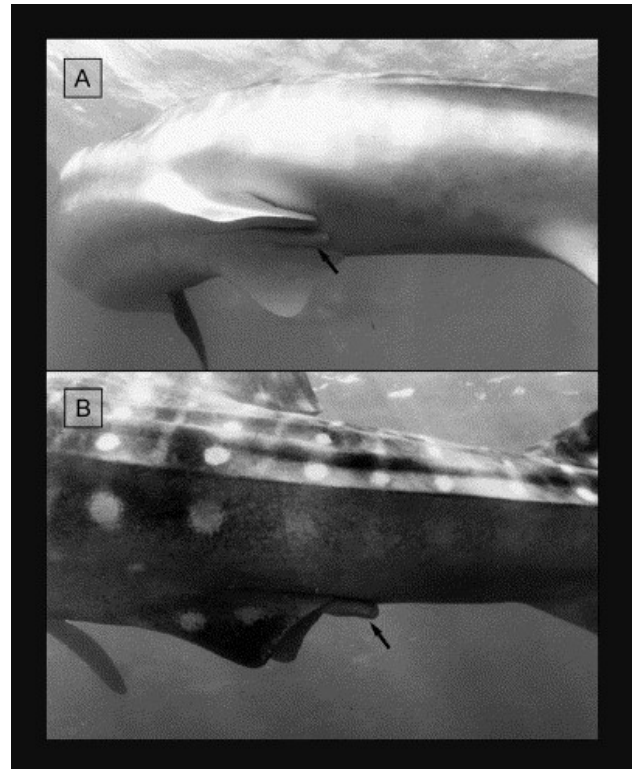
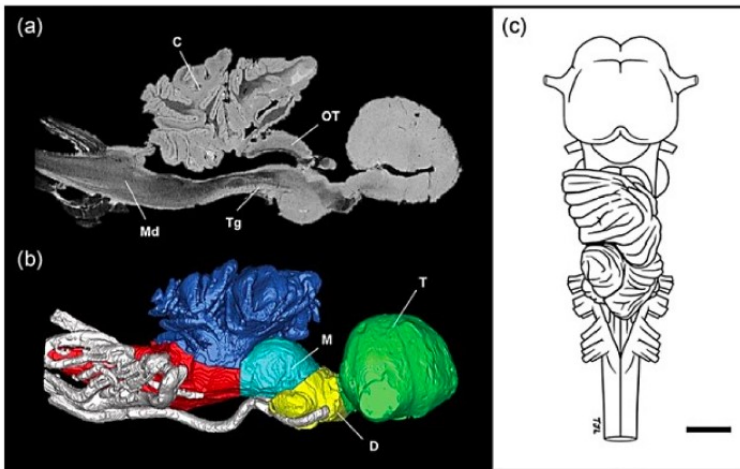


Figure 8 - Claspers of a male *R. typus*

Whale sharks have a slow growth rate with low population productivity, and they reach sexual maturity very late. Based on vertebral growth rings, Wintner (2000) found that a whale shark of ~5 m (precaudal length) would be approximately 20 years of age (Norman & Stevens, 2007). Studies suggest that the sexual maturity in both males and females may not occur until the sharks are over 9m in TL (Colman, 1997). Males are considered mature only if the claspers are fully calcified and their outer claspers' length is noticeably longer than the pelvic fins' length (Figure 8). In females, it is not possible to determine sexual maturity by simple external observation; the condition of the ovary and the width of the uteri are used as indicators of maturity. Fecundation is internal and the sperm is carried by the claspers into the reproductive tract of the female (Wintner, 2000).

1.1.9 Nervous system

Whale sharks present a brain of small dimension compared to their large body size. This has been hypothesized to be related to the feeding behavior, passive and opportunistic, characteristic of filter feeding which requires a lower activity compared to active predators (Yopak & Peele, 2021).



Nonetheless, the cerebellum of *R. typus* is extremely developed and stratified (Figure 9) to probably allow the great control in swimming movements both vertically and horizontally in the water (Yopak & Peele, 2021).

Figure 9 - The brain and its major regions of *R. typus*

Source: Yopak & Peele, 2021

1.1.10 Digestive system

The digestive system of sharks begins at the orobranchial cavity which consists of the mouth and the pharynx (Leigh et al., 2017). In whale sharks on both sides of the mouth five filtering

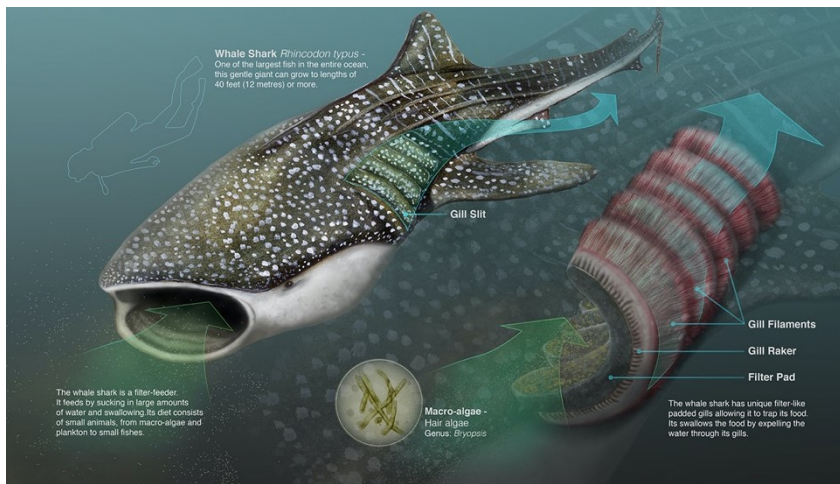


Figure 10 - Filter feeding process of *R. typus*.

Source: <https://cdna.artstation.com/>

pads are present (Figure 10), and the last one opens on the esophagus which is a short tube that transports food to the stomach. In general, sharks have a large J-shaped stomach for the digestion of proteins (Motta & Wilga, 1995).

The stomach connects to the intestine which is divided in 3 different regions: proximal, spiral, and distal intestines. This last region includes the rectum and feces are excreted into the cloaca (Leigh et al., 2017).

The stomach connects to the intestine which is

1.1.11 Circulatory system

The heart of fish consists of two cavities, one atrium and one ventricle arranged in series behind the gills. The aorta is elastic to regulate the blood flow that goes to the gills. Moreover, the pericardium is semi-rigid, and the pressure is always negative and lower than the atrial one to allow rapid filling during ventricular systole (Sherwood et al., 2012).

1.1.12 Sensory system

The sensory system of *R. typus* is highly developed to allow it to navigate the open ocean and to find prey. Moreover, it has been observed that whale sharks, as well as other shark species such as lemon sharks (*Negaprion brevirostris*) (Tuma, 1976); are able to use multiple sensory systems simultaneously and switch between them hierarchically as they approach a stimulus (Gardiner, 2014).

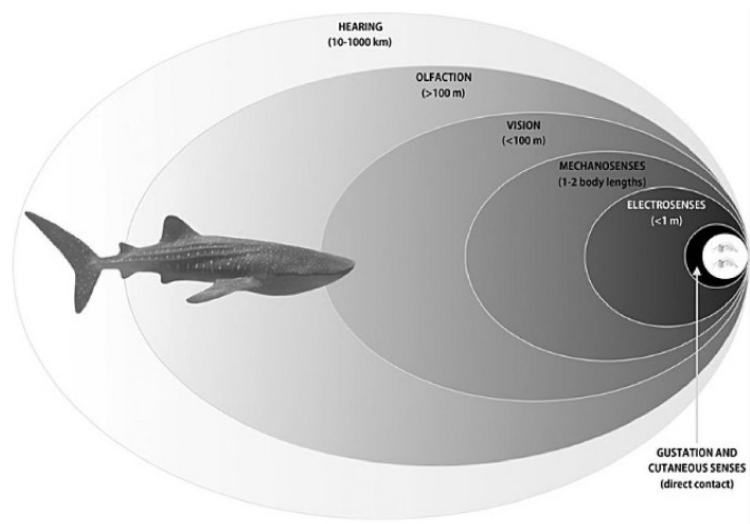


Figure 11 - Detection distance of each sensory modality of *R. typus*

Source: Yopak & Peele, 2021

When a whale shark is in proximity of a zooplankton patch, hearing, olfaction, and the electromagnetic senses are the most used in guiding the animal towards the prey. Whale sharks switch from one feeding behavior to another (for example they would switch from active surface ram feeding to passive feeding if the amount of food particle dramatically decreases) to maximize energy gain from the food source and minimize energy loss from not useful movements (Yopak & Peele, 2021).

For each sense there is a “detection distance” over which each modality is primarily used. Hearing system is the sense used from the greatest distance because sounds can be detected from thousands of kilometers away. Olfactory system is the second sense used for distance and smells can be detected from over 100m away. The third sense is vision system, which can be used up to 100m and mechanoreception of the lateral line is able to be used from 1 to 2 body

lengths away from the animal. The electrosensory system can be used from 1m to 30cm from the stimuli and taste sense only upon contact (Figure 11) (Yopak & Peele, 2021).

1.1.12.1 Hearing system

Hearing system is one of the first cues used by animals when hunting for prey because sound travels further in water. Sound is also used for other activities such as finding mates, avoiding potential predators, and long-distance navigation. Whale sharks present the largest inner ear of the entire animal kingdom (Figure 12) (Muller, 1999), it is anatomically like other vertebrates composed by three canals filled with fluid and presents a tiny crystal called otoconi which direct the head movement to maintain orientation and equilibrium in water (Fay & Popper, 1980). Even if the hearing sensitivity range of whale sharks has not been studied, sharks in general have a higher sensitivity towards hearing lower frequencies between 40 to 1000 Hz (Casper & Mann, 2009).

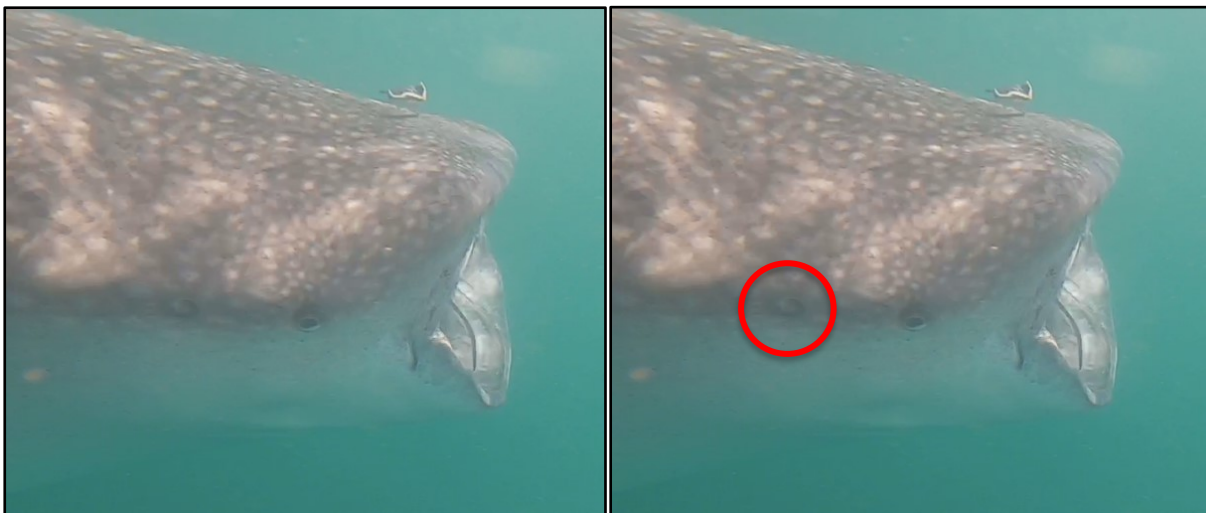


Figure 12 - Left: head of *R. typus*. Right: in the red circle it is highlighted the ear of *R. typus*

Source: photo by Pietro Storelli, a team member, Djibouti 2022.

Relevant observations have been made during a study in Honduras near the island of Utila where *R. typus* was often sighted near *Thunnus atlanticus* feeding locations. It has been suggested that the noise produced by the fish jumping when hunting for zooplankton was detected by whale sharks feeding on tuna eggs and other fishes associated with tuna enough to attract them to the location and take the chance of finding spawning animals (Fox et al., 2013).

1.1.12.2 Chemoreception

In sharks the chemosensory system is composed of two senses: olfactory and taste senses. An odor can be detected given the property of smell to travel in water very easily. The capacity of the shark to sense it also depends on the movement of water and the speed at which the animal is traveling (Yopak & Peele, 2021).

Olfactory system

Chemotaxis is the term used to describe the sharks' ability to orient and navigate towards a smell. The external olfactory system is composed of the nasal openings called nares and barbels which are small extensions of skin below the nasal openings (Figure 13). Inside the nares the olfactory epithelium is composed of primary and secondary folds also called olfactory rosette which increase the surface area to detect odors.

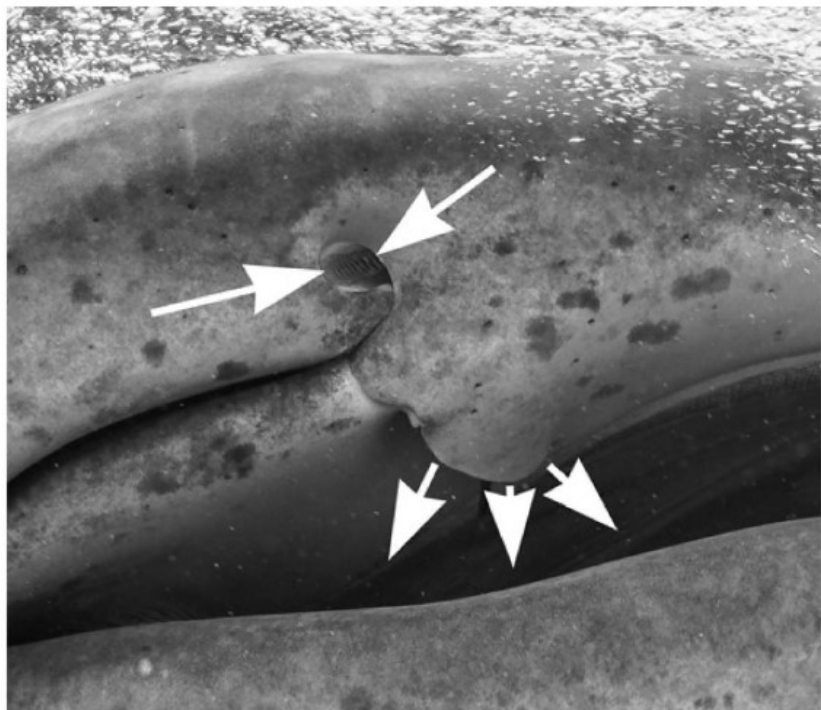


Figure 13 - The nares, showing water flow pattern.

Source: Dove, Georgia Aquarium

Once the water carrying the odor reaches the nasal openings, it flows into them and passes over the olfactory epithelium. Here the odor can be detected by olfactory receptor neurons which send the information to the brain. The water then flows below the barbel to finish into the mouth (Yopak et al., 2015).

In whale sharks, nares are located at the external margin of the upper jaw.

It has been speculated that whale sharks have evolved the olfactive abilities to locate zooplankton by detecting dimethyl sulfide, DMS. This substance is produced by phytoplankton when they are hunted by zooplankton, so it is an indirect method for whale sharks to detect the presence of food (Rohner & Prebble, 2021). It has been observed in captive whale sharks that they respond to chemosensory cues from both krill and dimethyl sulfide. Moreover, whale sharks may be able to sense DMS both in the water and in the air just above the water as it is suggested by the position of their nares and the upper jaw during active surface ram-feeding (Dove, 2015).

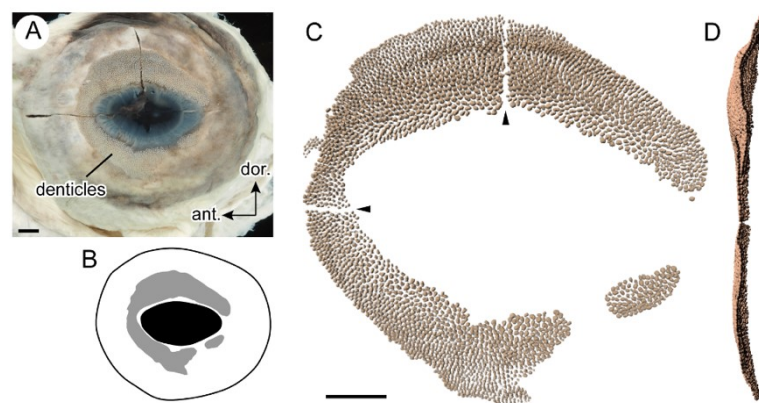
Taste system

Sharks in general have taste buds covered with receptor cells within papillae in the mouth and gills. Moreover, the frontal part of the mouth has the highest concentration of buds, leading scientists to believe that biting the prey is key for determining palatability. Unfortunately, no research has been done on the whale sharks' taste system, bud density or capability and much work needs to be done (Yopak & Peele, 2021).

1.1.12.3 Vision system

Light detection is fundamental for the visual system, which can be used by sharks at a distance up to 100m. Eye size in sharks is related to the environment they live in, but whale sharks have small eyes compared to the body size. This may reflect the fact that they do not rely on visual cues when finding food and feeding (Yopak & Peele, 2021). Moreover, whale shark eyes are positioned laterally on the extremities of their head, giving them almost a 360° view which can be increased by the sinusoidal swimming compensating for blind spots in front of the head (Yopak & Peele, 2021). A

unique adaptation of whale sharks is that they do not possess a nictitating membrane to protect the eyes, but the surface of their eyeball is covered by denticles probably to reduce abrasion of the ocular surface (Figure 14) (Tomita et al., 2020).



doi: <https://doi.org/10.1371/journal.pone.0235342.g002>

Figure 14 - Armored eyes of *R. typus*. A. Distal view of the left eyeball. B. Distribution of the eye denticles. C. Three-dimensional image of eye denticle aggregation. D. Posterior view of panel.

Source: Tomita, 2020

Whale sharks have circular pupils which are associated with species that do not live in environments with large fluctuations in light intensity (Hart et al., 2006). Moreover, they seem to have a rod dominated vision, which means they do not possess a high discrimination of colors; therefore, this species does not rely on visual cues for locating and capturing prey (Yopak & Peele, 2021).

An interesting study done by Hara et al. (2018) pointed out that the light sensitivity of *R. typus* is shifted towards the blue spectra. This may be related to the fact that they are the deepest diving fishes and often migrate towards the bathypelagic zone (Hara et al., 2018).

1.1.12.4 Electroreception

The electrosensory system works only when the shark is in proximity with other organisms, and it detects the electric stimuli produced by them (less than 5 nV/cm). Again, this system in whale sharks has not been studied but it can be inferred that, based on the lifestyle and feeding behavior, they have few pores located on the head in order to detect the plankton more easily (Yopak & Peele, 2021). This system has been largely studied in other species of elasmobranchs and it is generally used to find prey, avoid predators, and help with conspecific communication. Moreover, electroreception can be used for geomagnetic navigation actively or passively: the first is used by following the currents and the latter by using the earth's magnetic field to direct the movements (Yopak & Peele, 2021). The system is composed of receptors called Ampullae



of Lorenzini (Figure 15) which are located underneath the dermis and embedded in the ampullary canal. Canals are filled with hydrogel which enhance the voltage gradient and are lying with sensory receptor cells (Yopak & Peele, 2021).

Figure 15 – Highlighted the Ampullae of Lorenzini on *R. typus*.

Source: Warren Baverstock, wetpixel.com

1.1.12.5 Mechanoreception

Mechanoreception in whale sharks is used to detect the large water currents used for migrations, navigation, and orientation to nutrient-rich locations to feed. They also can detect the small water currents generated by other organisms in the water (Yopak & Peele, 2021). The lateral line system is what mechanically enables the shark to detect the water movements. Even though the lateral line system of whale sharks has not yet been studied, there are many studies on related sharks that can give us an insight on its functioning.

The lateral line system is composed of a series of sensory organs located on the side of the body of the animal from the head to the tail. When it is stimulated by movements of the animal or the water, hair cells move and stimulate the nerve cells sending a message to the brain. The brain processes the signal and obtains accurate information about the velocity, frequency, intensity, and location of the change of pressure (Yopak & Peele, 2021).

1.2 Diet

Whale sharks are planktivorous animals and studies have demonstrated that they feed on zooplankton such as Copepods (Figure 16) and on preys that tend to aggregate in dense patches (Rohner & Prebble, 2021). In the Gulf of Tadjoura (Djibouti), the Sharks Studies Center-Scientific Institute of Massa Marittima (GR) has conducted a preliminary study on the zooplankton size structure. The results highlighted the presence of 59 species of zooplankton, with 80% composed of Copepods during the day, which shifted to 47% at night. Other taxa were represented by Chaetognatha, Ostracoda, Thaliacea, Amphipoda, Pteropoda, and Sergestid (Di Capua et al., 2021). In the Nosy Be (Madagascar) area, 14 mesozooplanktonic phyla were identified, with again the majority represented by Copepods, followed by Appendicularia, Mollusca, and Chaetognatha (Bava et al., 2022).



Figure 16 - Left: Zooplankton aggregation. Right: Copepod.

Source: left: a-z-animals.com, right: algaebar.com

The peculiarity of *R. typus* is highlighted by the fact that it lives and feeds in warm waters where the plankton productivity is lower compared to where other planktivorous shark species live and feed (Rohner & Prebble, 2021).

In general, feeding is energetically expensive for *R. typus* because the hydrodynamic profile is broken by the open mouth and drag increases. Moreover, the different feeding mechanisms adopted also have a different energy consumption. In fact, whale sharks only feed when the biomass of the prey present is abundant enough to have an energy gain. This is the limiting factor influencing whether the shark feeds or not (Rohner & Prebble, 2021).

Larger whale sharks have a more differentiated diet compared to smaller individuals. It is also true that smaller sharks are often seen on coastal areas and larger sharks are rarely observed, suggesting also that adult sharks may be more specialized and better hunters able to feed at depths where the zooplankton aggregations are smaller and less dense (Rohner & Prebble, 2021).

In addition, a study conducted by the Sharks Studies Center in the waters of Nosy Be (Madagascar) has highlighted that the biomass of zooplankton sampled in the area was two orders of magnitude lower than the minimum energy requirements by whale sharks, hence it was not energetically sufficient to alone sustain young whale sharks (Bava et al., 2022; Marsili et al., 2023). This result suggests the possibility that whale sharks feed not only on zooplankton, but also on multiple prey sources such as tuna, anchovies, and mackerels which could be the primary target of whale sharks (Bava et al., 2022; Marsili et al., 2023). In addition, the presence, and levels of some chlorinated xenobiotics (HCB, DDT and its metabolites, and PCBs) were evaluated in order to estimate the possible impact of whale shark diet on organochlorine (OC) accumulation, highlighting that the daily contamination input of *R. typus* individuals, depending on their plankton diet, was minimal (Marsili et al., 2023), therefore supporting the hypothesis that the zooplankton biomass sampled in this region was not sufficient for the sustenance of the animals.

Given the gentle nature of this species and the fact that they feed at the surface has allowed scientists to study their diet. There are three direct methods used to analyze prey items:

1. Plankton collection: it is a simple and cost-effective method, but it is not possible to state if the shark ate all the species present in the mesh or only some of them. This method is also limited to coastal surface areas and to daytime (Rohner et al., 2015).

2. Stomach content analysis: it is a more direct method and even if it has never been done on whale sharks, it gives the certainty of the species ingested both during the day and at night. The problem is that the animal must be killed or researchers need to use stranded animals to analyse its stomach (Rohner et al., 2015).
3. Fecal analysis: collection and analysis of fecal samples is a non-invasive method, but it is difficult to find and collect samples (Rohner et al., 2015).
4. Stable isotopes analysis: through the skin-biopsy technique offers an alternative method for investigating diet and trophic level occupied by sharks in the food chain. This technique is minimally invasive, and it can provide, through the analysis of the ^{15}N stable isotope in the skin, the type of prey ingested and assimilated by the animal over a specific period and the trophic level occupied by the shark in the food chain (Borrell et al., 2011).

1.3 Feeding behaviors

To ingest the highest possible amount of prey and to spend the lowest amount of energy, these animals have evolved specific feeding strategies which depend on the density of zooplankton present in the water (Nelson & Eckert, 2007):

- “ram (or passive) -feeding”: in this technique the shark has the mouth partially closed and it is swimming forward (Figure 17) (Taylor, 2007). By doing so, particles in the water are ingested thanks to the locomotion and the gills are not pumping. This technique is used when the density of prey is low, small, or not moving (Nelson & Eckert, 2007).



Figure 17 - *R. typus* ram (or passive)-feeding
Source: photo by Lara Maule, Djibouti 2022

- “suction feeding”: the shark is in vertical or diagonal position in the water, with the tail sinking towards the bottom and the mouth forms a vortex at the surface of the water to suck prey which are actively ingested (Figure 18) (Rowat & Brooks, 2012). This mechanism is used when patches are small, and sharks also feed on small fishes.



Figure 18 - *R. typus* suction feeding

Source: photo by Lara Maule, Djibouti 2022

- “active surface ram-feeding”: when this technique is used, the animal is swimming at the surface of the water with most of the dorsal part of the body outside of the water and the mouth wide open (Figure 19). This feeding behavior is observed when there is a high density of prey (Rowat & Brooks, 2012).



Figure 19 - *R. typus* active surface ram-feeding

Source: photo by Lara Maule, Djibouti 2022

Once the shark has ingested a large amount of prey, they need to clean the gill rakers from debris and they perform a movement that resembles an underwater cough (Taylor, 2007).

1.4 Movements

1.4.1 Horizontal Movements

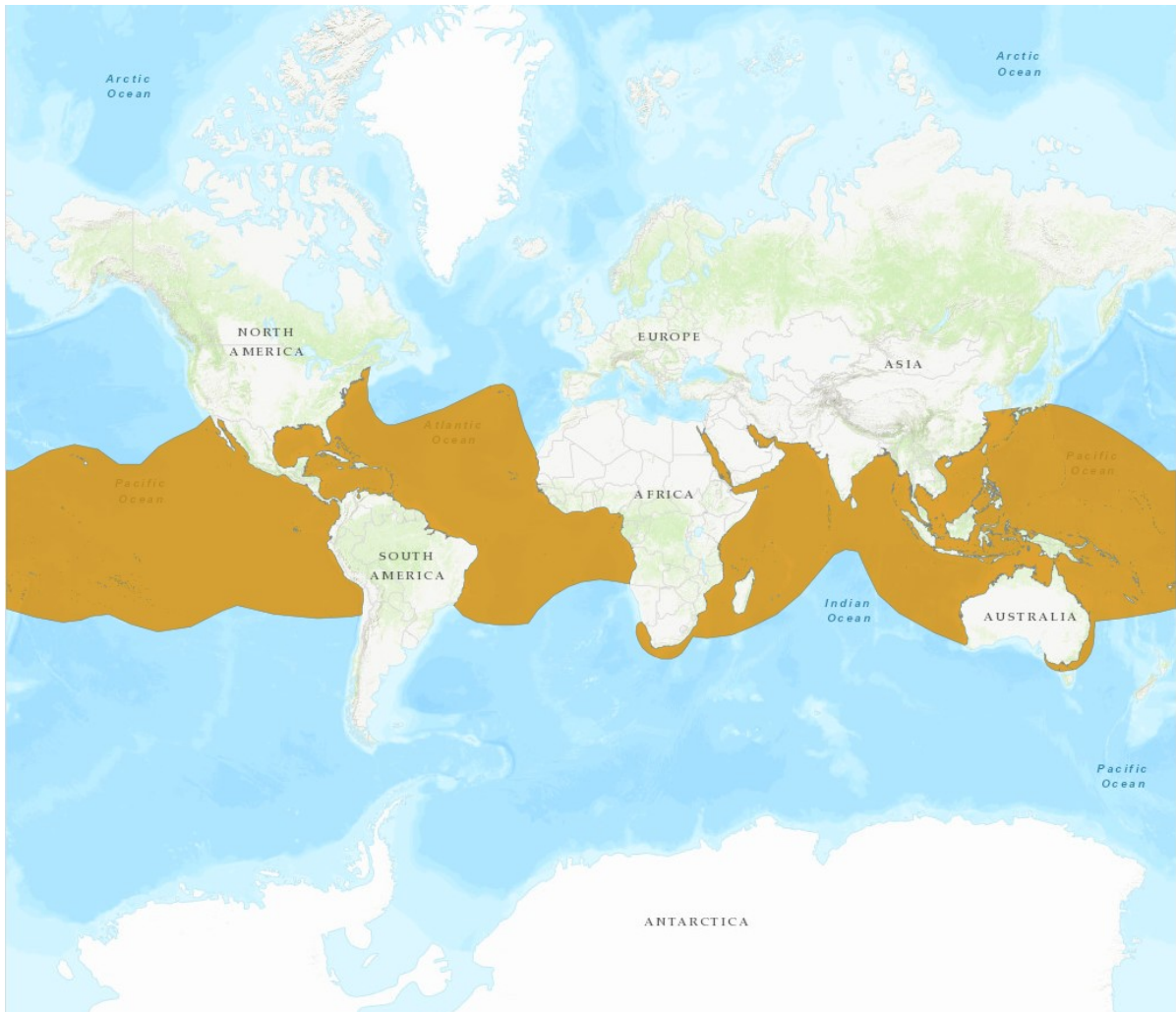


Figure 20 - *R. typus* distribution range

Source: iucnredlist.org

R. typus is a highly migratory species which can migrate long distances to areas of localized blooms of planktonic species. Studies have demonstrated that they are also capable of transoceanic movements (Hueter et al., 2013). Their geographic range is composed mainly of tropical and warm waters (Figure 20). Whale sharks can show a significant degree of site fidelity, but most sharks tagged to analyze their movements were immature males and they tend to aggregate at the surface. It is very rare to find new-borns, sharks smaller than 3m TL or larger than 10m; in fact, the observations and studies are immature male-based aggregations and not a real representation of the entire populations of sharks (Robinson et al., 2017).

1.4.2 Vertical movements

Whale sharks are known to be the deepest diving fish, and their vertical depth range therefore is very wide and goes from the epipelagic zone to depths of 1928m. (Tyminski et al., 2015). *R. typus* is an ectothermic species and it can control the temperature of its body only behaviorally, meaning that they need to swim to warmer or cooler areas depending on their body temperature. It has been observed with satellite tagged whale sharks that they spend some time in the warmer surface waters after returning from a deep dive, possibly to warm up (Robinson et al., 2017).

1.5 Threats

The whale shark is listed by the IUCN (International Union for Conservation of Nature) Red List as “Endangered” with the last assessment published in 2016 (Figure 21) (Pierce & Norman, 2016), and it was listed as “largely depleted” in the Green List in 2021 (Pierce et al., 2021). *R. typus* became legally protected under Appendix II of CITES (Convention on International Trade in Endangered Species) in 2002 (CITES, 2003). Appendix II includes species not necessarily threatened with extinction, but in which trade must be controlled in order to avoid utilization incompatible with their survival. Unfortunately, the number of individuals in populations has been decreasing since 2003. The major threats for these animals have been observed to be the collision with small and large vessels causing scarring and wounds whereas large vessels may be the cause of “cryptic” mortalities (Womersley et al., 2021). They are also commonly caught as bycatch and captured in the nets of fisheries (Pierce & Norman, 2016). Another threat is indirectly caused by the ingestion of microplastics when the animal is feeding. Once ingested, this material decreases the assimilation of nutrients, physiological processes, and reproductive fitness (Reynolds et al., 2022).

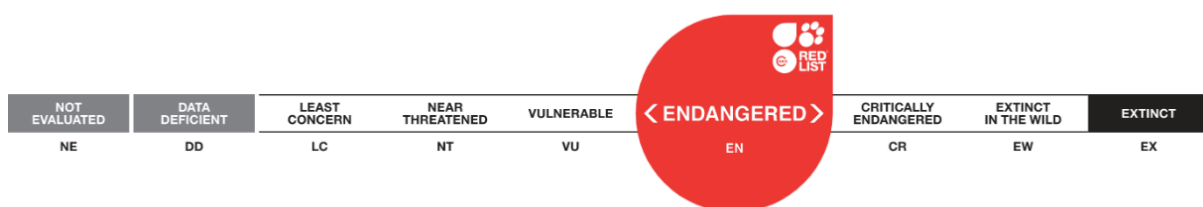


Figure 21 – *R. typus* IUCN red list category and criteria.

Source: iucnredlist.org

1.6 Conservation strategies

To date, many countries have adopted conservation strategies towards *R. typus*: Australia, Belize, Djibouti, Honduras, India, Maldives, Mexico, Philippine, Seychelles, Taiwan, Thailand, and U.S.A (Rowat & Brooks, 2012).

The first conservation strategy was implemented in 1982 by the *United Nations Convention on the Law of the Sea* (UNCLOS), but it was not directly protecting whale sharks. It was implemented to monitor fishing activities and those activities that were directly impacting the oceans. In 1995, the whale shark was included in the *United Nations Agreement on Straddling and Highly Migratory Fish Stocks* (UNCDFMFS), but there were no practical actions to guarantee the conservation and management of this species. In 1998, the *Food and Agriculture Organization of the United Nation* (FAO) was the first to publish a Plan of Conservation and Management of Sharks, which led to the publication of the National Plans of Action. In the year 2000, *R. typus* was added to the Red List of the IUCN as “Vulnerable”, listed into the *Convention of Migratory Species of Wild Animals* (CMS), and into the *Convention on International Trade in Endangered Species* (CITES). These conventions were the first to directly protect the species globally forbidding the fishing and regulating the trade of the species (Rowat & Brooks, 2012). Since 2010, the whale sharks have also been included in Annex I of the CMS Memorandum of understanding on the Conservation of Migratory Sharks (Sharks MOU), which has been signed by 48 countries (CMS 2020b) The Sharks MOU is a legally non-binding instrument that aims to facilitate favorable conservation status for migratory sharks (Pierce et al., 2021)

1.7 Ecotourism

Ecotourism is defined by the International Ecotourism Society as “Responsible travel to natural areas that conserves the environment and sustains the wellbeing of local people” (TIES, 2003). Over the last decade, ecotourism has increased around whale sharks, becoming one of the fastest-growing sectors in marine wildlife tourism. This shift was possible thanks to the peculiar characteristics of this species: docile giant, predictable presence, and accessibility (Ziegler & Dearen, 2021). These new tourism activities should first and foremost benefit sharks. By raising awareness, it is possible to incentivize the creation of laws to improve conservation, involve the local communities, and protect other species that live in close contact with whale sharks. Moreover, tourism brings higher financial benefits than the extraction of the animal (Ziegler & Dearen, 2021). One throwback for these activities is maintaining the health of animals: it has been observed that 93% of tourists do not respect the minimum distance from the shark which

may cause distress in the animal and modification to the feeding behaviors. In fact, sharks that had more visits to a specific site in the Philippines were more likely to suction feed in a steady position. Moreover, these sharks were also accustomed to anthropogenic stimuli, indicating habituation (Legaspi et al., 2020).

Nowadays there are many sites where it is possible to observe non captive whale sharks in the wild. One of these sites is the Gulf of Tadjoura in Djibouti, and this thesis could have not been written without the development of ecotourism activities in that area. The main income of the local population was obtained from fishing but, over the past years, it is shifting towards ecotourism with whale sharks being the main attraction. This is important for the local population because the financial gain is much higher and less physically demanding than fishing. Sharks benefit as well because they are now protected, and conservation awareness is increasing (Figure 22).

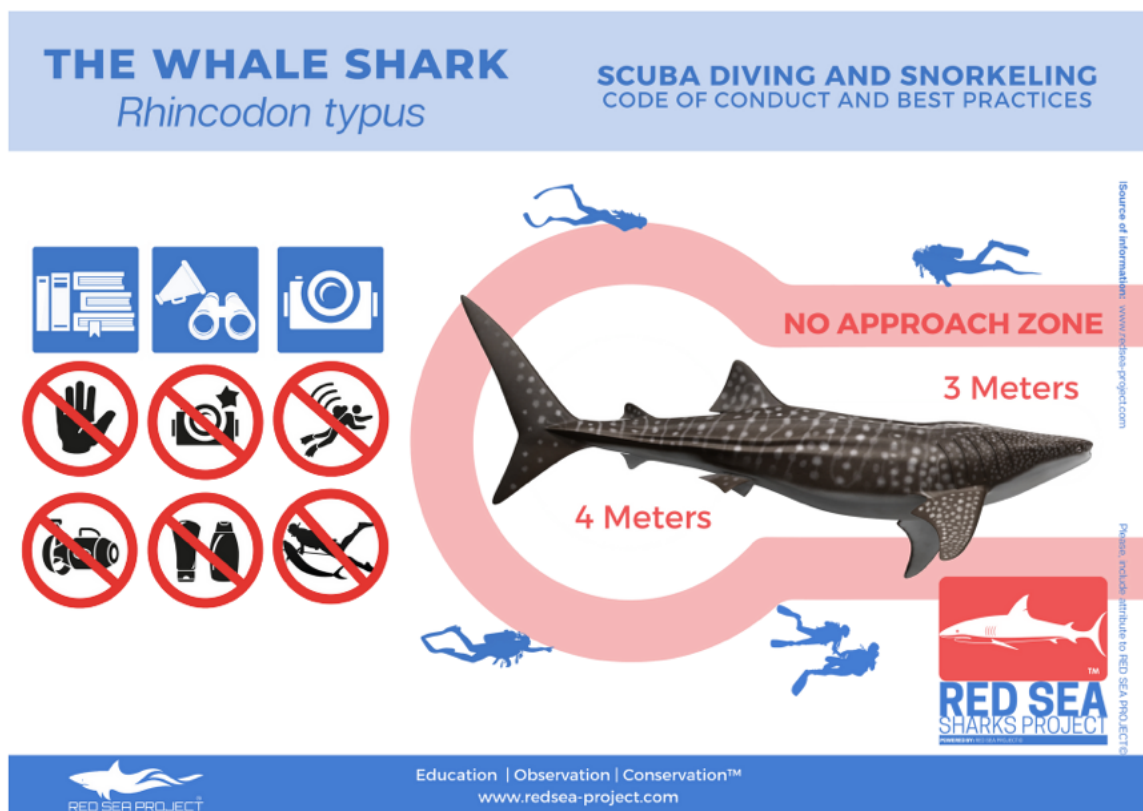


Figure 22 - Code of Conduct when interacting with *R. typus*.

Source: redsea-project.com

2. Material and Methods

2.1 Sampling areas

The Sharks Studies Center has been working on the ecology and ethology of whale sharks since 2017 in two areas: Djibouti, and Nosy Be in Madagascar (Micarelli et al., 2022). In these areas the Sharks Studies Center team carried out 4 expeditions in each site (2017, 2020, and two in 2022 in Djibouti; 2017-2018-2019-2022 in Madagascar). This thesis is focused just on the Djibouti area where I collected my data.

Djibouti

The scientific expedition to which I participated in Djibouti took place in November 2022. The republic of Djibouti is a country located in east Africa, bordered by Eritrea in the north, Somalia in the south, Ethiopia in the southwest and the Red Sea in the east.

Djibouti is in the Horn of Africa, on the Gulf of Aden and the southern entrance of the Red Sea. The climate is mostly desertic and temperatures are above 35°C from May to October. From October to May they oscillate between 23°C and 30°C. The water temperature is between 25°C and 28°C (Copernicus.eu).

The expedition coordinated by the Sharks Studies Center took place in Arta Bay (11°35'38,4" N, 42°49'37,0" E), and Ras Koralı (11°34'27,7" N, 42°46'24,1" E) (Figure 23).



Figure 23 - Map of Djibouti. In the red circle is highlighted the area where the expedition was located, and the data collected.

Source: www.mapsofworld.com

2.2 Methods

Data Collection

The expedition's group in November 2022 was composed of 8 people: 6 students and 2 coordinators from the Sharks Studies Center. The group was hosted for 5 days on the 25m sailboat "Elegante" (Figure 24) which was harbored in the gulf of Ras Korali. The research activity's schedule was composed of two daily excursions: from 9:00 to 11:00, and from 16:00 to 18:00. The group was brought with zodiacs to the areas where whale sharks were known to be seen to increase the probability of sighting.

Sharks were sighted mostly from the experienced skipper of zodiacs who was able to locate the dorsal fin of the animals at the surface far away. While the zodiac approached the shark at a safety distance, members of the groups were getting ready to enter the water. Each member of the expedition was equipped with a mask, snorkel, fins, and an action-cam for underwater videos. Once the shark was nearby, the team descended into the water slowly and quietly, following the protocol set up by the Sharks Studies Center to avoid disturbing the individual.

Underwater videos were taken by the group at the safety distance, trying to have in one video both sides of the animal, and scars or unique signs which could be used to identify the animal. Moreover, in each trip, two members of the team used the laser photogrammetry equipment to estimate the TL of the animal.

Each video was then analysed after each trip by members of the team at the end of the day. The analysis consisted of filling out an identification sheet for each animal sighted. The first aim was to find in the videos the left and right side of each shark, record the position of sighting, the sex, when possible, record the date, the video and photo references, and in the comment



Figure 24 – Sailboat "Elegante" where the expedition took place.

Source: photo by Enrico Vittorini, a team member, Djibouti 2022

section both the feeding activity of the animal and marks or scars on the animal were recorded as well.

2.3 Photoidentification

To study species' biology, ecology, and demography, one of the requirements is to correctly identify and recognize individuals. One of the easiest ways to do so is to use natural markings characteristics of species (e.g., color patterns, scars, scratches, etc.). The use of video recording of animals in their natural habitat, with little to no disturbance, represents an alternative or supplement to conventional invasive tagging techniques (Marshall & Pierce, 2012).

Whale sharks are one of the best examples where this technique can be applied, for several reasons: they present a unique pattern on the dorsal part of the body which may present only minor changes over the years (Arzoumanian et al., 2005) and it is a calm and easily approachable species, so it is easy to take videos and photos even without the use of diving equipment.

I³S Classic photoidentification software

I³S stands for Interactive Individual Identification System. This photoidentification software is adapted from an algorithm developed within the astronomical community for stellar pattern recognition. Digital images were matched using the computer program *I³S* (Van Tienhoven et al., 2007), which is an effective tool for semi-automated photoidentification of whale sharks (Speed et al., 2007). *I³S* allows to 'fingerprint' the spot patterns on the skin of a whale shark and compare these to similarly fingerprinted images in the database to see if the shark has been previously photographed.




This technique was developed from another software used for stellar pattern recognition and it presents 4 different versions depending on the pattern to be recognized/matched: *I³S* Classic is used for whale sharks and sand tiger sharks *Carcharias taurus* (Rafinesque, 1810); *I³S* Spot is used for manta rays; *I³S* Pattern is used for sea turtles, and *I³S* Contour is used for whales. All the programs work in a similar way and help the operator, through pictures, to highlight the pattern of animals and to compare it to the ones present in the database. Two outcomes are possible: if the software finds a match, the animal is already present in the database; if there is no match, the individual is new and can be added to the database. It is important to point out that there must always be an operator to verify if the match is exact.

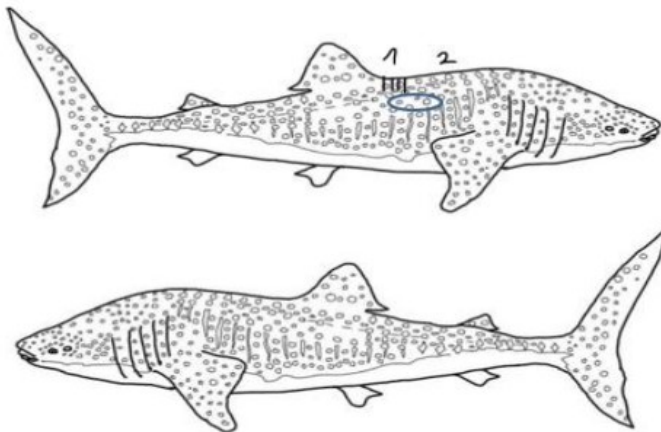
The process to analyze images through the *I³S* software follows precise steps:

1. The videos of whale sharks are analyzed and the best frame representing the area between the 5th gill slit and the pectoral fin is extrapolated, since it is the part that present minors' changes over the years (Arzoumanian et al., 2005).
2. The frame is uploaded on *I³S* Classic, and it is verified if the individual is a new sighting, in which case it is added to the database and a number is assigned to it. If the individual is already present in the database, it is marked as a resighting.
3. Once the individual is identified, an identification sheet is filled out for each of them. In the sheet it is present the left and right picture of the animal (used for the photoidentification in *I³S*), the identification number, date, and coordinates of the sighting (using the GPS location), the sex of the animal, when possible, the TL, feeding behavior, and any scars or peculiar signs which could better characterize the individual (Figure 25).

Rhincodon typus Smith, 1828



Left side	Shark ID	Right side
	DJ 2022 sch 19	
Date 16/01/2022	N° 19	Length 6,24 ± 0,1 m (laser)
GPS <u>N</u> 11° 35.298' <u>E</u> 042° 48.475'		
Video references N. Andraoi - "Esemplare 19 DJ 2022"		
Photo references		
Comments Durante il primo avvistamento (del 16-01-22), l'esemplare si è alimentato per 2 minuti in modalità <u>vertical suction</u> Riavvistamento del 17/01/2022		
Body marks 1: quattro tagli paralleli visibili sul lato destro, posizionati anteriormente rispetto la pinna dorsale 2: macchia/cicatrice bianca sotto i tagli (1)		
		



X=Scars

O=Others

Figure 25 - Example of a shark ID sheet of the individual number 19, sighted and recorded in Djibouti in 2022.

Source: Sharks Studies Center.

The I^3S program helps the recognition of individuals by comparing pictures already registered and marked in the database. For each picture, three blue points are plotted: one point at the top of the gill slit (first dorsal), another point at the bottom of the fifth gill slit (second dorsal) and the last point on the most-posterior point of the pectoral fin (pectoral). The software will insert a fourth point at the intersection between the first and third point to form an ideal rectangle. In this area the centre of the white spots of the shark's flank are marked with red dots. For a more precise identification, it is better to mark between 15 and 30 white spots (Figure 26). By marking the three reference points, the program can re-scale and rotate the images to allow comparison even if the photographer is not orientated in the best position to the shark (Van Tienhoven et al., 2007).

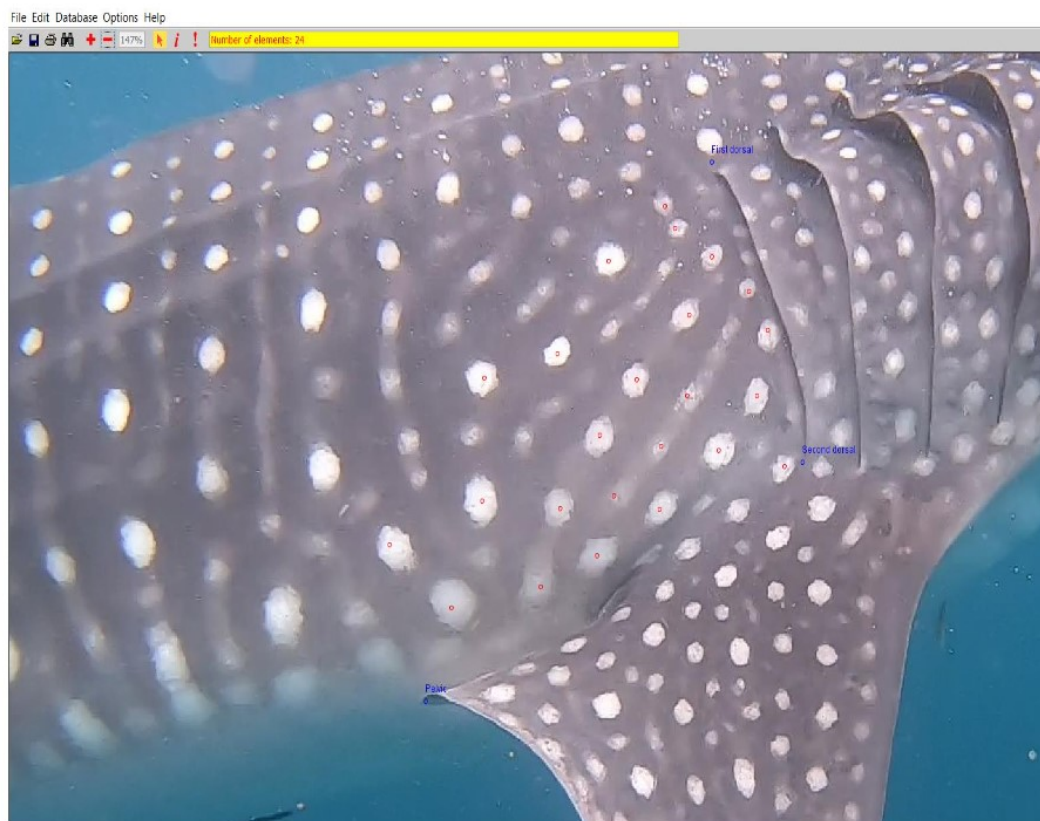


Figure 26 – Photoidentification of a whale shark through I^3S Classic program sighted in Djibouti in 2022. In the image are clearly visible the three blue spots used to define the photoidentification area and the red ones used to define the pattern that must be compared with the other ones just present in the database.

Source: Sharks Studies Center.

Finally, the frame is saved in the database and the program compares it to the ones already registered. The program *I³S Classic* gives a score to the match (Figure 27): if the score is 0.00 the animal is a perfect match with one already present in the database and it is marked as a resighting; a score ≤ 10.00 determines a reliable match, most certainly the animal is the same; a score > 10 and ≤ 20.00 requires the operator to manually and visibly check the two frames (the one from the database and the new one) to verify if it is a match or not; a score ≥ 20.00 are not considered.

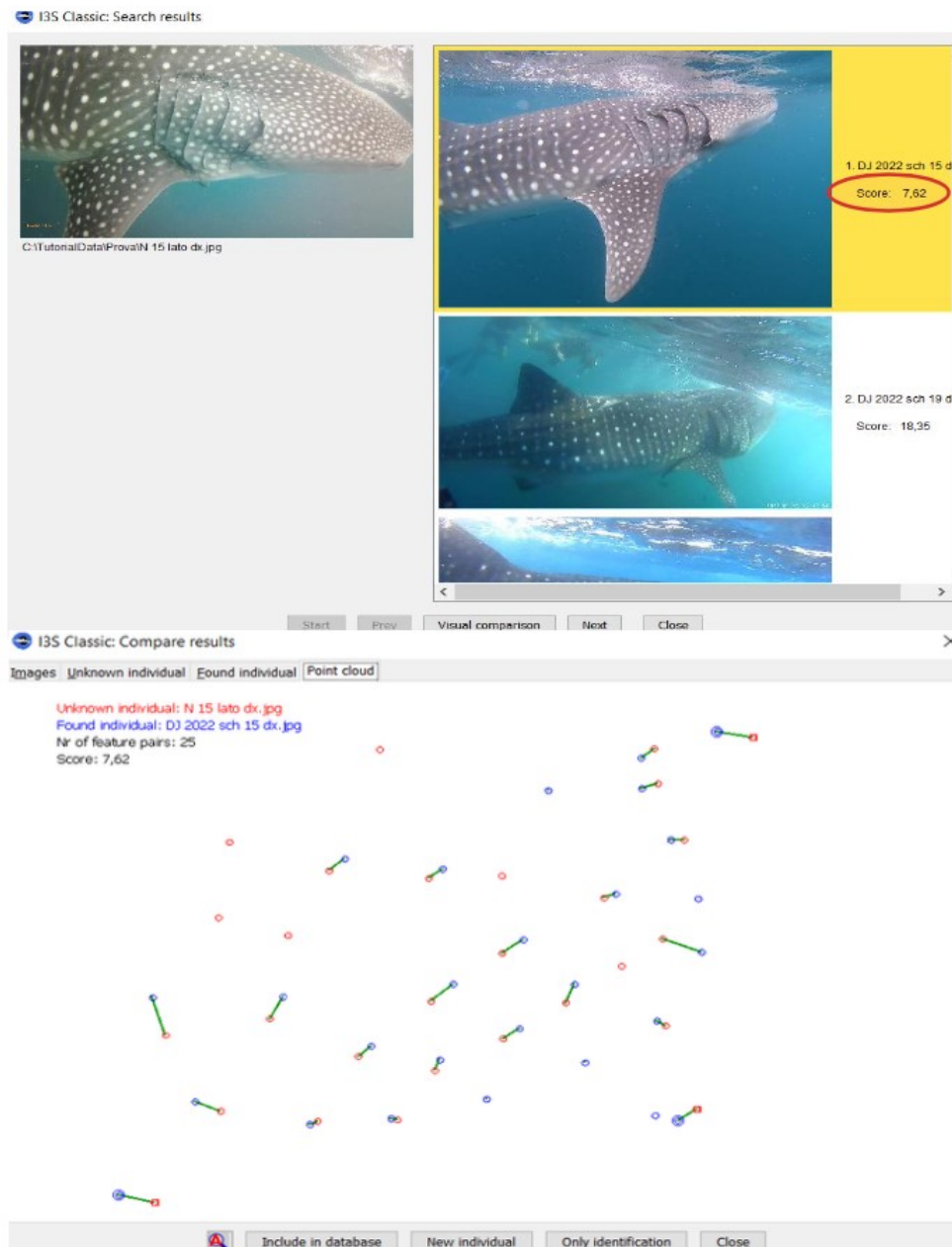


Figure 27– Comparison through I³S Classic of two different photos of the sample n. 15 sighted in 2022 in Djibouti. The score is 7.62 between the two photos, indicating that it is the same shark.

Source: Sharks Studies Center.

It is important to point out that this photoidentification technique, despite having very reliable results, is not internationally recognized due to errors that may occur because of the difficulties given from underwater filming of moving animals:

- The frame must be free of any element that could cover the identification area (light reflexes, air bubbles, and other animals swimming around the whale shark).
- The pectoral fin cannot cover the identification area.
- If the underwater camera presents a wide angle or a 360° setting, the structure of the animal is distorted, and the identification area is compromised.

These problems may not be recognized by the software and consequently one individual may be saved twice in the database as two different individuals because there is no match between the pictures; or it can bring to discard a new individual because of an apparent likeness with an individual already registered. Moreover, the program is not universally recognized also for the fact that it highly relies on the presence of an operator to plot the dots and to decide, depending on the score of animals matched, if the shark analysed is a resighting or not.

2.4 Laser-photogrammetric survey

Laser-photogrammetry is the second approach used in this thesis and it is used to measure the TL of a shark. The device is composed of 5 main pieces: a flat and solid base, a handle, 2 green lasers placed at 30cm of distance and parallel from each other, and a camera placed in the middle of the lasers (Figure 28). During the observation of sharks, the camera is turned on and it is pointed towards the side of the animal, between the first dorsal fin and the head. A video is recorded perpendicular to the animal, and it is important that the

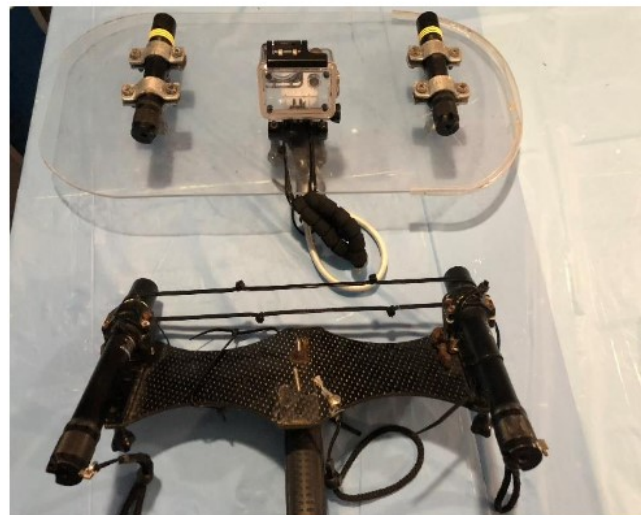


Figure 28 – Laser-photogrammetry device used to measure the TL of the sharks.

Source: Sharks Studies Center.

operator is close enough and that the two lasers can be visible from the video, together with the

tip of the roster and the beginning of the dorsal fin. The color of the laser used for this method must be green because it is easily visible underwater.

The protocol for the laser-photogrammetry to estimate the measure of whale sharks follows these steps:

1. Once the video is recorded, it is analysed on a computer.
2. The best shot, with all the necessary points, is screenshots. The four reference points must be visible on the frame: the two lasers' dots on the side of the animal, the tip of the roster, and the first dorsal fin (Figure 29).

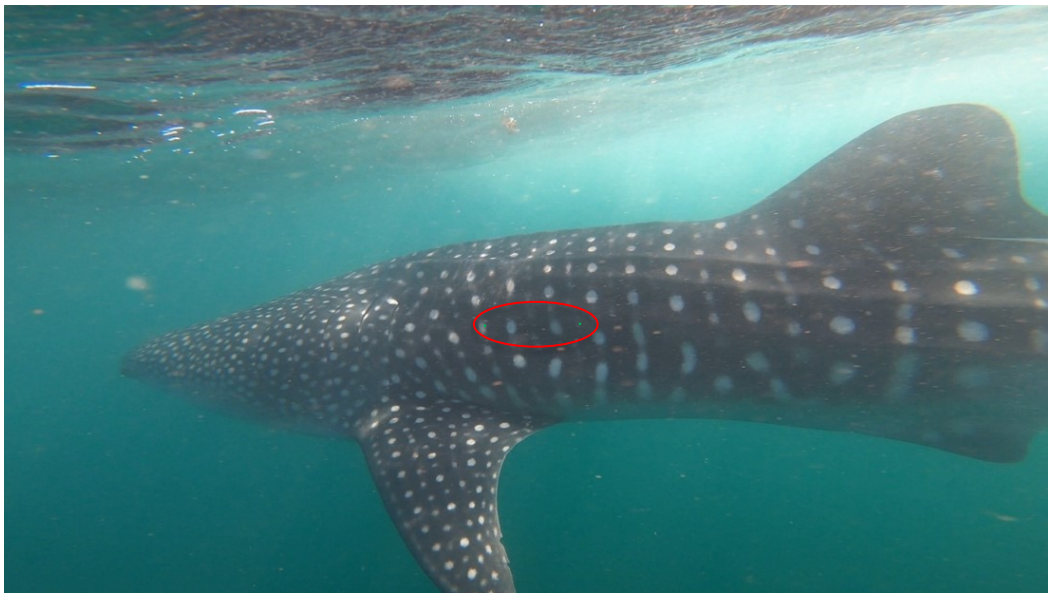


Figure 29 - Frame chosen to measure the individual number 37, Djibouti 2022; the two green pointers of the laser are clearly visible.

Source: photo by Lara Maule, Djibouti 2022

3. The picture is examined with the digital software “Paint”: one line is traced between the two laser’s points (reference segment, 1); another line is traced between the roster and the first dorsal fin (subject segment, 3). Line number 2 (segment 2) is traced starting from the base of the first dorsal fin perpendicular to the intersection with line 3. The horizontal pixels are recorded at the two extremities of the line segment for each of the two lines (1, and 3) (Figure 30).

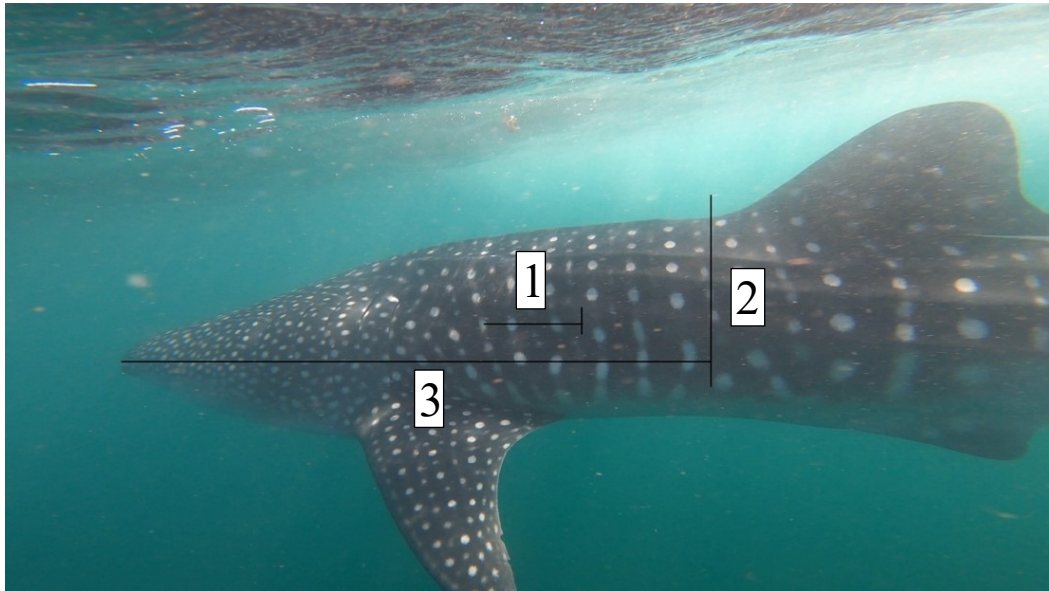


Figure 30 - Frame examined with “Paint” of the individual number 37, Djibouti 2022.
 1, line between the two pointers of the laser. 2, perpendicular line starting from the dorsal fin. 3, line from the roster to the perpendicular line to point 2.

Source: photo by Lara Maule, Djibouti 2022.

4. The horizontal pixels of the reference segment (1) are subtracted, and the value corresponds to 30cm (distance between the lasers points).
5. The horizontal pixels of the subject segment (3) are subtracted.
6. At this point with the proportion (a) it is possible to calculate the length of the individual between the roster and the first dorsal fin.

$$(a) \quad \text{ref} : \text{subj} = \text{pixref} : \text{pixsubj}$$

Therefore:

$$\text{subj} = (\text{ref} * \text{pixsubj}) / \text{pixref}$$

Where *ref* is the distance between the laser beams (30cm), *subj* is the subject that is measured, *pixref* is the number of pixels between the laser and *pixsubj* is the number of

pixels between the roster and the first dorsal fin. The values are calculated by an excel sheet by copying the formulas every time a picture is processed.

In this way, the measure obtained is referring to the part of the shark between the roster and the first dorsal fin. If it was possible to have in one frame the TL of the animal, and the lasers pointers to be visible, by using the same proportion the TL could be measured. Given the large size of this animal, it is not possible to increase the distance from the individual because the laser pointers will be lost.

To obtain the TL of the animal it is essential to use the Matsumoto et al. (2017) calculation:

$$\text{Log TL} = 0.964 * \log \text{subj} + 0.433$$

So, through “Excel”, it is possible to obtain the measure of each shark in meters with an error between 1.4 and 3.3% (Matsumoto et al., 2017). In the excel sheet, all the formulas listed above, the number of pixels of the reference segment, and the subject segment are plugged in, and the final measure in meters is calculated automatically (Figure 31).

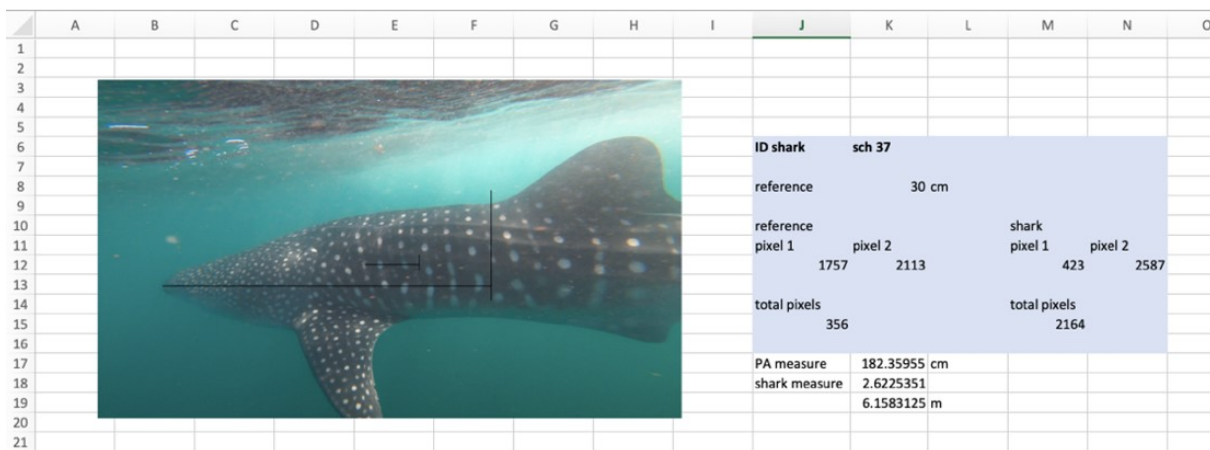


Figure 31 - Final measure of the individual number 37, Djibouti 2022.

Source: photo by Lara Maule, Djibouti 2022

2.5 BORIS

The Behavioral Observation Research Interactive Software (BORIS) is an easy-to-use event logging software for video/audio coding and live observations of animal behaviors. It has many functions, and the program allows the calculation of time-budgets and provides statistics for the duration, occurrence, and intervals of the events.

BORIS is a free and open-source software available for GNU/Linux, Windows, and MacOS. (BORIS v. 7.7.3; Friard & Gamba, 2016). This software was used to analyze the videos of sharks when feeding to create ethograms and datasets for further statistical analysis.

In the software the names of all the animals recorded during the years were inserted and the ethogram for the feeding behaviors was created. The steps to analyze one video are:

1. Upload the video from the folder to the software and name it by the name in the folder to avoid confusions (each video should be called as the name of the individual in it).
2. Change the time and date if it was recorded.
3. Start the observation by pressing the key on the keyboard corresponding to the name of the animal.
4. Start the video and record the behavior by pressing the key on the keyboard corresponding to the behavior of the animal (a: active surface ram-feeding, p: ram (or passive)-feeding, and s: suction feeding).
5. Once the video is finished, save the project, and start another video (Figure 32).

Once all the videos are visioned and analyzed, many outputs can be extrapolated from BORIS. For this thesis, the transition matrices were exported to create ethograms and the data were also exported on an “Excel” file and divided by day, individual, and type of behavior observed.

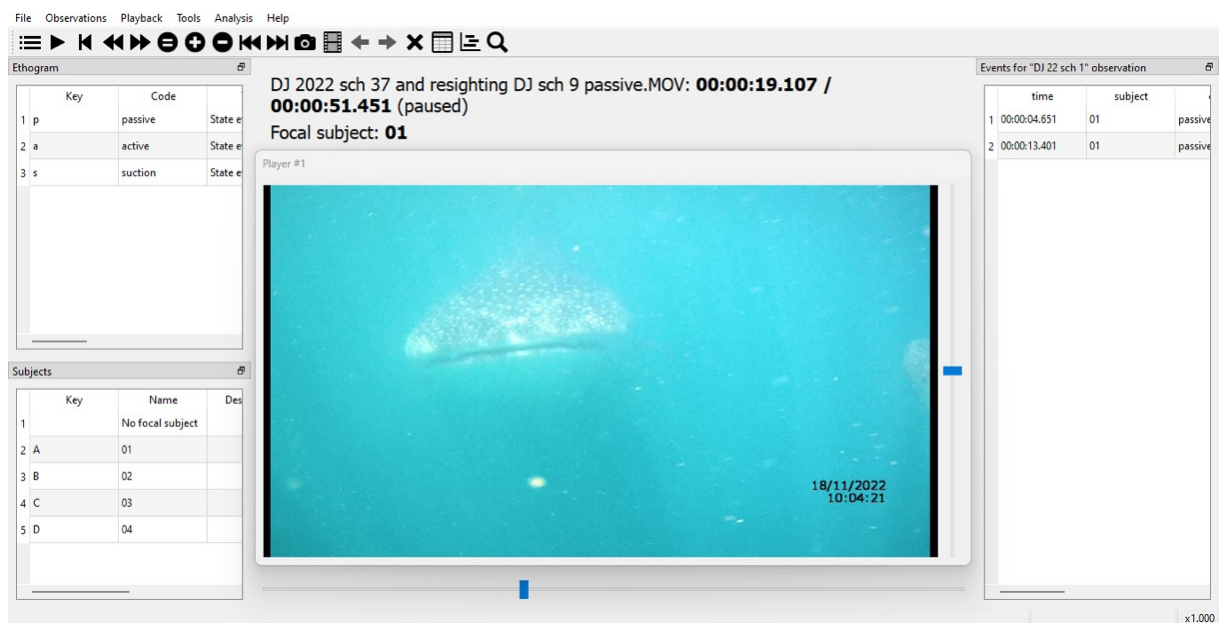


Figure 32 - Example of BORIS analysis

Source: Lara Maule

2.6 Collection of Environmental data

Environmental data are parameters which can highlight and allow evaluation of variations in the environment when an event needs to be measured. It is necessary to use multiple sets of data because each of them gives a specific information (www.isprambiente.gov.it).

Environmental data were collected during all the scientific expeditions carried out in Djibouti (2017, 2020, 2022) and during each exit to the sea with zodiacs.

For this thesis, environmental data taken in consideration were:

- A. Light levels, expressed in OKTAS, collected always by the same operator. It is a unit of measurement used in meteorology to measure cloudiness of the sky, estimated in terms of how many eights of it are obscured by clouds (Rees, 2001). Measurement intervals used to assess the sky coverage were as follows:
 - a) 0-2 oktas corresponded to clear sky.
 - b) 3-5 oktas corresponded to partly cloudy sky.
 - c) 6-8 oktas corresponded to a totally covered sky.
- B. Sea conditions, taken from the windguru database for Djibouti area (www.windguru.cz). The conditions were categorized in calm, slightly rough, and rough according to the Douglas scale of wave height.
- C. Surface water temperature, expressed in Celsius degrees (C°), was collected from the Copernicus database (www.copernicus.eu).
- D. Wind speed, expressed in knots, was collected from the windguru database for Djibouti area (www.windguru.cz).
- E. Rainfall, expressed in millimeters per hour (mm/h), was collected from the windguru database for Djibouti area (www.windguru.cz).
- F. Time of the day, expressed in hours (h), was calculated by the exits to the sea done with zodiacs during each day in all the expeditions (scheduled times: 09.00-11.00; or 16.00-18.00).
- G. ENSO, expressed in multivariate ENSO index MEI, means El Niño Southern Oscillation and is the ocean-atmosphere phenomenon that causes global climate variability on interannual time scales. It was recorded from the NOAA database (www.noaa.gov).
- H. Chlorophylls concentration, measured in milligrams per cubic meter mg/m³, was collected from the Copernicus database (www.copernicus.eu).

2.7 Statistical analysis

This study focused on five main research questions: (1) to prove that the whale sharks' behavior was potentially affected by endogeneity issues because of not directly observed factors (named omitted variable biases) and not directly measured variables (named unobserved heterogeneity); (2) to investigate the main factors related to sea conditions and climate change affecting the whale sharks' behavior; (3) to assess the existing relationship (whether it matters) among environmental conditions; (4) to evaluate in detail how environmental factors affected the recorded behaviors; and (5) to investigate whether the number of sightings over the time was potentially affected by ENSO measurement unit, evaluated according to the Multivariate ENSO Index (MEI).

The dataset analysed in this study contained both not directly and not observed factors to deal with endogeneity issues. The former corresponded to six environmental factors: (i) light levels, measured in oktas; (ii) surface water temperature, measured in Celsius degrees (C°); (iii) rainfall, measured in millimetres per hour (mm/h); (iv) wind speed, measured in knots; (v) ENSO measurement unit, evaluated through the Multivariate ENSO Index (MEI); and (vi) concentration of chlorophylls, measured in milligrams per cubic metre (mg/m³). Concerning not directly measured variables, they have been computed as *proxy* discrete variables and consisted of two additional environmental parameters: (i) sea conditions in terms of sea activity as ordinal variable, assuming values 1 (whether the sea is calm), 2 (whether the sea is slightly rough), and 3 (whether the sea is rough); and (ii) time spent during the sightings as *dummy* variable equals to 0 (time slot 9:00-11:00) and 1 (time slot 16:00-18:00). The variable of interest corresponded to the whale sharks' behavior. It was computed either as *dummy* variable equals to 0 (ram (or passive) - feeding behavior) and 1 (active surface ram - feeding and suction feeding behaviors) to be estimated in the logistic function or as ordinal variable equals to 1 (active surface ram - feeding), 2 (ram (or passive) – feeding behavior), and 3 (suction feeding).

The dataset was further arranged to better analyse the degree of interdependence and/or relationship between not directly and not observed factors. More precisely, some variables have been grouped in classes and then evaluated as categorical or ordinal discrete indicators. They were: surface water temperature, assuming values 0 for the class < 26 C° and 1 for the class ≥ 26 C°; rainfall, assuming values 0 for the class 0.0 mm/h and 1 for the class > 0.0 mm/h; wind speed, taking values 1 for the class 3.0–6.9 knots, 2 for the class 7.0–9.9 knots, and 3 for the class 10.0-12.9 knots; MEI, assuming values 0 for the class between -2.1 and 0.0, and 1 for the class between 0.1 and 2.0; and concentration of chlorophylls, taking values 1 for the class 0.00-

0.50 mg/m³, 2 for the class 0.51-2.00 mg/m³, and 3 for the class 2.01-more mg/m³. Every group of classes has been computed based on its median on the sample size (250 sightings), so that each class was equally distributed and weighted when making inference.

The first three questions were addressed through a multiple step procedure, named Three-Step System Multivariate Classification (TSMC), over 250 sightings and three time periods (2017, 2020, and 2022). More precisely, the TSMC consisted of:

- (i) computing a Permutational Multivariate Analysis of Variance (PERMANOVA) to evaluate dissimilarity degree (or dispersion) when comparing heterogenous groups of factors (first step);
- (ii) estimating a logistic regression to study the relationship between a variable of interest and a set of predictors (second step);
- (iii) computing sample marginal effects to investigate the main predictors (or covariates) affecting the outcomes of interest (third step).

First step: Permutational Multivariate Analysis of Variance (PERMANOVA)

Concerning the PERMANOVA analysis, the null hypothesis refers to homogeneity (equivalent dispersion among groups) while the alternative one when a relevant dispersion matters among groups (heterogeneity). Before running the PERMANOVA, a correlation matrix was performed to investigate potential collinearity problems occurring when highly strong correlation among two or more predictors occurred. Generally, in non-linear models, the threshold used is a correlation function $\geq 40\%$.

The main aim in this first step was to study the degree of relationship (in terms of dispersion) among factors and outcomes of interest. The estimates have been obtained according to the robust Aitchison distance by Martino et al. (2019) to make them applicable to all non-negative data including zero (unlike the standard Aitchison). The reason stands for the presence of several categorical variables and then the risk to incur in a *dummy* variable trap. The latter refers to the case in which two or more columns/rows of the matrix containing the predictors are equal between them (linearly dependent vectors), making impossible to estimate the related regression parameters.

The set of covariates was defined as a $n * k$ matrix X , where $i = 1, \dots, n$ and $j = 1, \dots, k$ denoted the units and the variables, respectively. There were 9 variables so labelled: 'okta', denoting light levels; 'sea', referring to sea conditions; 'ntemp', describing surface water temperature; 'nwspeed', describing wind speed; 'nrain', denoting rainfall; 'ntime', denoting the time slot scheduled during a sight; 'nenso', referring to MEI; 'nchlorop', denoting the

concentration of chlorophylls; and ‘year’ referring to the time period. The outcomes of interest, in this step, referred to ‘dbehavior’, denoting whale sharks’ behavior evaluated as a *dummy* variable.

Here, three main assumptions needed to be held: (i) objects in the dataset were exchangeable under the null; (ii) exchangeable objects (e.g., sites, observations, factors) were independent of each other; and (iii) exchangeable objects had similar multivariate dispersion across units.

Second step: Logistic Regression Function

Concerning the logistic regression, it corresponds to a non-linear probabilistic function useful to regress a set of covariates on a discrete categorical (or *dummy*) variable of interest. The logistic regression function was evaluated to study in detail the results achieved in PERMANOVA analysis. Here, we recalled that the variable of interest denoting the whale sharks’ behavior has been computed as a categorical variable: =1 active surface ram - feeding/suction feeding and =0 ram (or passive) - feeding. The connection between active surface ram – feeding and suction feeding behaviors was because the latter would mean that the whale shark was inclined to assume a sort of ‘active behavior’.

The logistic function was expressed as:

$$(1) y_i = \sum_{j=1}^k X_{ki} \gamma_k + \varepsilon_i$$

where $n = 250$, X_{ki} referred to the matrix containing all predictors evaluated in the first step, γ_k were the regression parameters to be estimated, and ε_i denoted the error term (or causal component).

Finally, before computing and compare (sample) marginal effects for every predictor across units over time, a discriminant analysis was performed. This latter focused on selecting the ‘best’ submodel solution (or combination of predictors) to predict the variable of interest and avoid potential (multi)collinearity problems among strictly correlated predictors (just as in this study), where ‘best’ referred to the subset of predictors better fitting the data. The estimating procedure takes the name of Best Subset Selection (BSS) analysis and consists of building and, in turn, comparing several possible regression models based upon an identified set of covariates. The ‘best’ submodel solution corresponds to the one with the lowest Bayesian Information Criterion (BIC). The BSS and the logit regression are classified as Machine Learning (ML) algorithms.

Third step: Sample Margin Effects

Let the logit model estimate in equation (1), the (sample) marginal effects were computed as:

$$(2) \frac{\partial F(X_{ki}\gamma)}{\partial x_{ki}} = f(X_{ki}\gamma) * \gamma_k$$

where x_{ki} denoted each predictor accounted for.

In this context, let strong correlation matter among covariates, Odds Ratios (OR) have been computed for each predictor evaluating the probability of an event favourable to an outcome. They correspond to the exponential of the estimated regression parameters $\hat{\gamma}_k$, and their related probabilities are computed as $(1 - OR) * 100$. The usefulness of using OR in terms of probability is because of: (i) strong correlation between predictors underestimating the (sample) marginal effects; (ii) multivariate classification based on discrete variables; and (iii) property of the probabilities assuming values 0 up to 1, according to the possibility to reach infinite values in case of (multi)collinearity problems.

Fourth step: Confusion matrices

The fourth question was performed through appropriate visualization tools, known in literature as confusion matrix. It corresponds to a performance measurement for ML classification algorithm. In this study, it was applied for multiclass classification problems based on the estimates achieved in the BSS analysis. An advantage of the confusion matrix is the ability to compute the predictive capability to verify the accuracy (or consistency) of the estimates achieved in a ML classification algorithm. In this section, we considered the variable of interest built as ordinal factor to understand how environmental factors affected every possible behavior and why whale sharks were inclined to assume active surface ram - feeding (A), ram (or passive) – feeding (P), or suction feeding (V) actions. According to the findings achieved in the multivariate classification algorithms (TSMC and BSS), a confusion matrix was then used for each of the main factors affecting whale sharks' behavior: 'nchlorop', 'okta', 'rain', and 'temp'. The last three predictors ('sea', 'nwspeed', and 'ntime') have been evaluated through ENSO measurement unit (MEI), discarded from the analysis because of strong correlation with them. In this context, surface water temperature and MEI were not considered grouped in classes to investigate any of their possible value. Every confusion matrix has been interpreted in terms of probability to better evaluate the results denoting the joint probabilities. The predictive capability is computed as: $1 - mean(\%)$, where the mean is obtained by the ratio between the outcomes on the main diagonal (representing the number of success and unsuccess) and the total observations.

All the findings obtained by means of the confusion matrices, recalling in turn the estimates obtained in the TSMC and BSS analyses, were confirmed by performing a Cochran's Q test. Indeed, the hypothesis testing referred to independency (or causal choice, under the null) between the whale sharks' behaviors and chlorophylls concentration or dependency (or not causal choice, under the alternative).

Fifth step: Influence of the ENSO phenomenon on the interannual whale sharks' sightings in Djibouti

The last insight was addressed by means of a Chi-square test of independence to investigate whether ENSO measurement unit (MEI) and sightings over time were dependent (alternative hypothesis) or independent (null hypothesis) between them. More precisely, the hypothesis testing assumes that the two variables ('year' and 'enso') are likely to be not related (independency under the null) or related (dependency under the alternative). The test statistic was computed as:

$$(3) \chi^2 = \frac{\sum_i \sum_j (n_{(i,l)} - \hat{n}_{(i,l)})^2}{\hat{n}_{(i,l)}}$$

where $n_{(i,l)}$ denoted the absolute joint frequency, where i and l are numerical indices referring to two discrete variables and $\hat{n}_{(i,l)}$ stands for the absolute joint frequency in case of independence.

3. Results

3.1 Photoidentification

Using the software *I³S Classic* for pattern recognition in November 2022, 10 new whale sharks were identified, bringing the total sharks number identified in Djibouti to 49 individuals recorded in the database of the Sharks Studies Center-Scientific Institute. More specifically, in 2017 and 2020, 6 sharks were identified respectively, for a total of 12 sharks; in January and November 2022, 27 and 10 sharks were identified respectively, for a total of 37 sharks.

In November 2022, 11 resightings occurred; of these, one individual was a resighting of January 2020, and 10 were resightings from January 2022.

Where it was possible to determine the sex of individuals, most of them were males (when two claspers were clearly seen and filmed in the pelvic area).

3.2 Laser-photogrammetric survey

Laser-photogrammetric survey was performed on 9 sharks out of the 21 (both new individuals and resightings) observed during the expedition of November 2022. Of these 9 sharks, 6 were resightings from the January 2022 expedition and 3 were new individuals of November 2022.

In Figure 33 is reported the total length (TL) of the measured whale sharks and the average value of 6.05 m for all the 9 sharks. The average TL of the 3 new sharks (medium darkness color in graph 1) was of 6.06 m. The largest individual was the number 24 (sch 24) with a TL of 6.34 ± 0.1 m and the smallest one was the number 20 (sch 20) with a TL of 5.87 ± 0.1 m; both these sharks were resightings from the January 2022 expedition. Moreover, 4 sharks measured in January 2022 were also measured in November 2022: the number 1 (sch 1) was reported to be 0.23 m smaller in November compared to the TL obtained in January; the number 11 (sch 11) was 0.28 m smaller in November compared to the TL obtained in January; the number 15 (sch 15) was 0.13 m larger in November compared to the TL obtained in January, and the largest was reported to be again individual number 24 (sch 24) and it was 0.22 m smaller compared to the TL obtained in January.

All the sharks, according to the TLs recorded, were immature individuals.

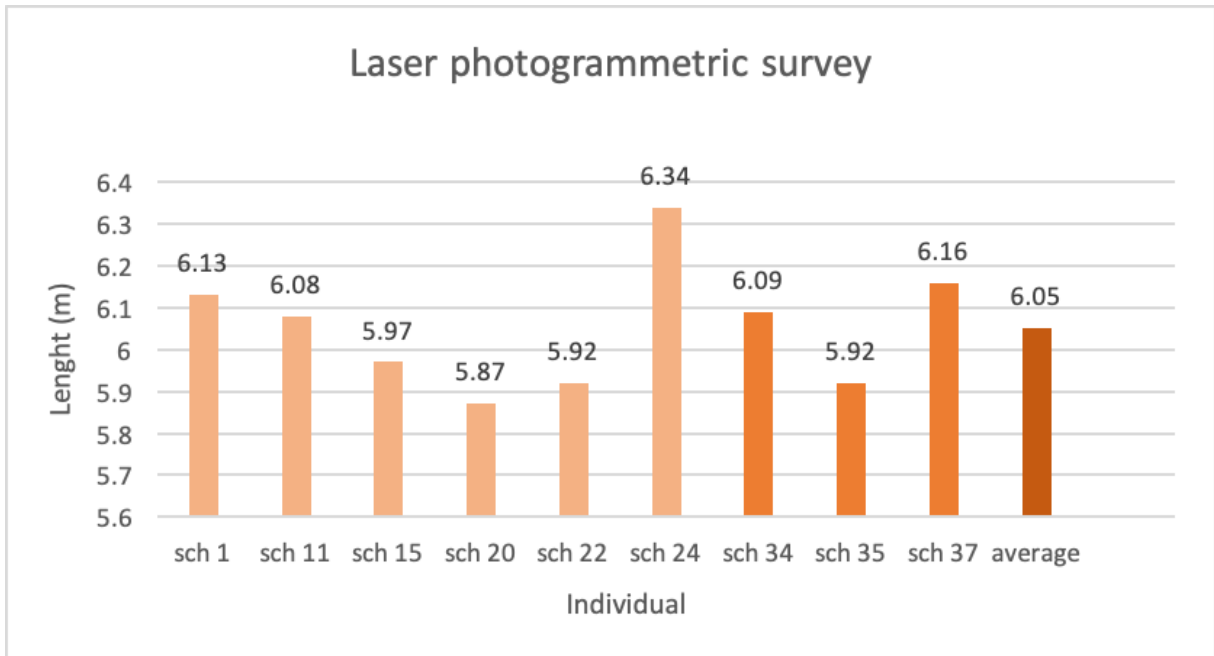


Figure 33 – Laser-photogrammetric measurements of 9 sharks. Sch 1, sch 11, sch 15, sch 20, sch 22, and sch 24 are resightings from the January 2022 expedition (lighter in color columns). Sch 34, sch 35, and sch 37 are new individuals observed in the November 2022 expedition (darker in color columns). The last column to the right shows the average TL of all the sharks measured (darkest color column) in November 2022.

3.3 Feeding Behaviors

The feeding behaviors recorded in November 2022, the results in Figure 34 showed that the feeding behavior with the longest time was suction feeding, followed by ram (or passive) - feeding and active surface ram – feeding (Figure 34). Regarding the other expeditions of the Study Sharks Centre, in 2017 the most seen feeding behavior has been ram (or passive)-feeding; in 2020 was suction feeding and in January 2022, ram (or passive)-feeding (figure 35).

Feeding behavior	Time (s)	Time (%)
Active surface ram-feeding	357.24	24.62%
Ram (or passive)-feeding	375.995	25.89%
Suction feeding	717.818	49.49%

Figure 34 – Total time in seconds (s) and percentages (%) of the feeding behaviors showed by the filmed whale sharks in November 2022.

Feeding behavior	2017	2020	January 2022
Active surface ram-feeding	14.01%	23.21%	19.88%
Ram (or passive)-feeding	54.91%	20.12%	44.56%
Suction feeding	31.08%	56.67%	35.56%
Total	100%	100%	100%

Figure 35- Percentages (%) of feeding behaviors for each expedition of the Sharks Study Centre.

In Figure 36, the results obtained showed that, in 2017, sharks switched more frequently from active surface ram-feeding to suction feeding and vice versa 28.6%. In 2020, the most frequent behaviors' change was from suction feeding to ram (or passive)-feeding (57.1%). In 2022 (January and November expeditions were analysed together being part of the same year), the most frequent behaviors' change was from active surface ram-feeding to ram (or passive)-feeding and vice versa (25%).

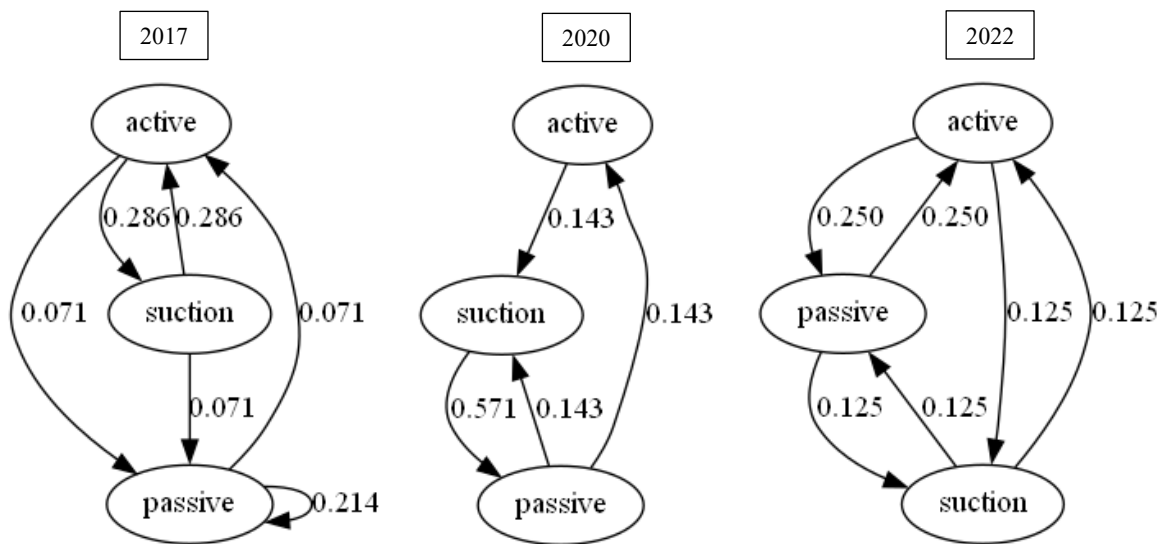


Figure 36 – BORIS ethograms output. On the left there are the frequency ethograms of 2017; in the middle of 2020, and on the right of 2022. The numbers refer to the frequency of behavior change for one shark for each year.

3.4 Influence of environmental factors on feeding behaviors and on interannual sightings of whale sharks in Djibouti

First step: Permutational Multivariate Analysis of Variance (PERMANOVA)

The correlation matrix has been performed to deal with potential (multi)collinearity problems let the predictors be strongly correlated between them (referring to similar events). The variables resulting strongly correlated with more than one predictor were ‘nens0’ (with ‘ntemp’, ‘nwspeed’, and ‘nrain’ displaying a correlation function $\geq 55\%$), and ‘year’ (with ‘sea’, ‘nens0’, and ‘nwspeed’ displaying a correlation function $\geq 40\%$). Thus, there have been dropped out, estimating overall 7 variables. The latter resulted significant at least at 10% as highlighted in the below estimation output (Fig. 37).

Source	Df	SS	Pseudo-F	Pr(>F)
okta	1	0.039	7.168	p<0.01 ***
sea	1	0.022	3.950	p<0.01 ***
ntemp	1	0.825	5.565	p<0.01 ***
nwspeed	1	0.189	4.985	0.06 *
nrain	1	0.185	5.521	p<0.01 ***
ntime	1	0.171	4.989	0.05 *
nchlotop	1	0.042	5.011	0.02 **
Residual	242	0.004		
Total	249	0.006		

Figure 37 - PERMANOVA analysis between environmental/climatic conditions and whale sharks' behaviors. Here, the labels stand for 'degrees of freedom' (df), 'Sum of Squared Dissimilarities' (SS), 'Pseudo F-statistic' (Pseudo-F), and 'associated p-value' (Pr(>F)). The significance levels are: (*) significance at 10%; (**) significance at 5%; and (***) significance at 1%.

Six considerations were in order. First, the predictor with highly larger Pseudo-F statistics and then high significance (1%) was 'okta' accounting for underwater visibility. Second, 'ntemp' and 'nrain' also achieved high significance even if with lower Pseudo-F statistics and larger deviance of residuals (or SS). It would be because of similar values collected in the dataset: surface water temperature and rainfall lined up on 25.9 °C and 0.0 mm/h on average, respectively. Third, the concentration of chlorophylls was significant (5%) even if displaying a low Pseudo-F test statistic (close to the one of 'nwspeed' and 'ntime' significant at 10%). It would be due to its strong dependency with weather and water conditions. For instance, the concentration of chlorophylls was positively correlated with visibility in terms of 'okta' (about 48%) and negatively with surface water temperature ('ntemp', about 55%). Fourth, wind direction ('nwspeed') and time scheduled during sightings ('ntime') showed similar results because of their positive correlation (about 55%). Fifth, sea conditions positively affected the outcomes $y=1$ (p-value close to zero), but with less Pseudo-F statistic. It would mean that the whale sharks' behavior was not strictly related to the sea conditions but, probably, to the presence of chlorophylls (positively correlated with water activity: worse sea conditions would decrease the number of chlorophyll). Indeed, even if rough sea showed more than 2,000 mg/m³, the data referred to 16 observations on 250 only. Finally, the residuals' Standard Errors were strictly close to zero, proving that the estimates were accurate (the analysis is efficient).

Second step: Logistic Regression Function

All predictors were significant at least at 5% except sea conditions (Fig. 38), highlighting the efficiency of the supervised ML algorithm minimizing the sum of squared residuals and that potential (multi)collinearity has been dealt with. Indeed, the full (or unrestricted) model, with all nine predictors, showed an Akaike Information Criterion (AIC) equal to 333.40, while the one of the restricted models (without ‘nens0’ and ‘year’) was equal to 311.89. The lowest AIC is the most preferred (restricted model).

Coefficients	Estimate	SE	z-value	Pr(> z)
okta	3.046	0.068	44.79	p<0.01 ***
sea	3.321	2.061	1.61	0.05 *
ntemp	-2.431	0.277	-8.78	p<0.01 ***
nwspeed	-1.240	0.541	-2.29	0.01 **
nrain	2.142	0.130	16.48	p<0.01 ***
ntime	-1.012	0.532	-1.90	0.03 **
nchlorop	3.248	0.057	56.98	p<0.01 ***

Figure 38 - Logistic regression functions analysing how environmental/climatic factors affect whale sharks’ behavior across units over time. Here, ‘Coefficients’ refers to the covariates; ‘Estimate’ refers to $\hat{\gamma}_k$ (the estimated regression parameters γ_k); ‘SE’ stands for Standard Error; ‘z-value’ denotes the test statistic obtained for each predictor (the ratio between ‘Estimate’ and ‘SE’); and ‘Pr(>|z|)’ refers to the associated p-value according to a two-sided hypothesis testing (where the null stands for non-significance). The significance levels are: (*) significance at 10%; (**) significance at 5%; and (***) significance at 1%.

Five main findings were in order. First, less visibility and stronger wind speed negatively affected the whale sharks’ behavior. It means that worse weather conditions would incline the whale sharks to assume a ram (or passive) - feeding behavior. It was an important result highlighting that the number of chlorophylls tends to decrease in case of worse weather conditions. Second, the predictor ‘nrain’ should be interpreted with care. Indeed, its positive effect would mean that an active surface ram - feeding behavior (including suction feeding) was preferred in case of more rainfall. However, the maximum mm/h collected during the sightings has been 0.1 and then it should be interpreted as: less rainfall was favoured with active surface ram - feeding (and/or suction feeding) actions, when the presence of chlorophyll would increase (because of the negative correlation between ‘nrain’ and ‘nchlorop’). Third, the negative effect of ‘ntime’ confirmed the PERMANOVA results. Let the positive correlation matter with wind speed, a worse weather condition during a sighting would favour a ram (or passive) - feeding behavior because of less chlorophyll. It highlighted again the highly positive dependency among active surface ram - feeding behavior (including suction feeding) and number of

chlorophylls. Fourth, an increase of water temperature negatively affected the whale sharks' behavior, favouring the ram (or passive) - feeding behavior ($y=0$), where the number of chlorophylls tends to decrease. Finally, sea conditions ('sea') positively affected the whale sharks' behavior ($y=1$), but with less significance (10%) due to its strong relationship with weather factors. By construction, higher values of 'sea' referred to worse water activity, and then an active surface ram - feeding/suction feeding behavior tended to be preferred in case of slightly rough sea.

Later, a BSS has been performed to better evaluate (and then confirm) the results achieved in the logistic regression. According to the Figure 39, the 'best' subset of predictors corresponded to the ones with lower BIC (positive values). More precisely, the surface water temperature would be relevant with outcomes ≤ 26.2 C°; the best subsets of chlorophylls, inclining the whale sharks to assume an active surface ram - feeding (or suction feeding) behavior, were associated with ≥ 0.60 mg/m³ (assuming values 2 and 3 by construction); rainfall with values ≤ 0.1 would be the best outcomes favouring the variable of interest ($y=1$); and ENSO measurement unit (MEI) lined up on ≤ -2.1 (good weather conditions). These findings confirmed and deepened the estimation results found in Figure 37. The 'nchlorop' with value 0.473 mg/m³, even if displaying more black squares than the values ≥ 0.60 mg/m³, has been discarded from the discriminant analysis because of its significance at highly larger BIC as well (from 23 to 51).

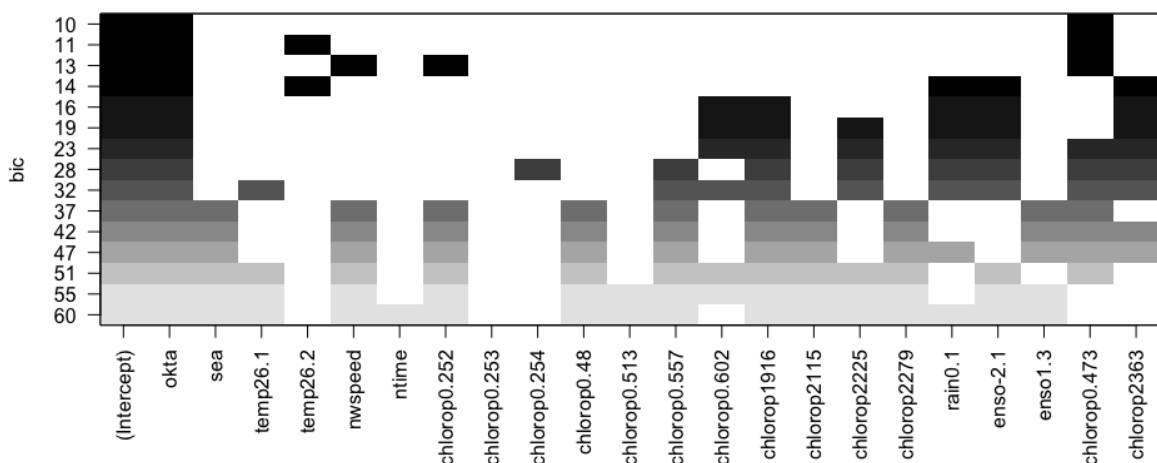


Figure 39 - Best Subset Selection shrinking procedure is assessed on the dataset accounting for all possible outcomes of each predictor. Here, 'temp' stands for water temperature; 'rain' denotes rainfall; 'chrolop' refers to the number of chlorophylls; and 'enso' stands for ENSO measurement unit (MEI). The black squares refer to stronger effect of every predictor on the outcomes of interest ($y=1$), corresponding to the lowest BIC (positive values).

Third step: Sample Margin Effects

According to the estimates displayed in Figure 40, the main factors affecting whale sharks' behavior, in order of importance, were: 'nchlorop' (75.18%), 'okta' (65.33%), 'nrain' (62.31%), 'ntemp' (56.89%), 'sea' (35.02%), 'nwspeed' (31.36%), and 'ntime' (28.76%). Between the brackets, there have been displayed the Odds Ratios (OR), and the results fully corresponded to the ones found in PERMANOVA analysis. However, an important consideration is that the predictor 'sea' would positively affect the whale sharks' behavior ($y=1$), but with not sufficiently high OR. This highlighted two findings: (i) sea conditions, according to the time periods, tended to assume value 2 (slightly rough) 'compromising' its estimate; and (ii) overall, worse sea conditions would incline the whale sharks to assume an active surface ram - feeding (or suction feeding) behavior. Finally, a White's heteroskedasticity correction test has been performed to standardize the residuals dealing with potential (multi)collinearity problems.

Coefficients	dF/dx	SE	z-value	Pr(> z)
okta	0.410	0.151	2.71	p<0.01 ***
sea	0.273	0.133	2.05	0.02 **
ntemp	-0.398	0.168	-2.37	0.01 **
nwspeed	-0.253	0.121	-2.09	0.02**
nrain	0.353	0.171	2.06	0.02 **
ntime	-0.192	0.110	-1.75	0.04 **
nchlorop	0.402	0.136	2-96	p<0.01 ***

Figure 40 - Sample marginal effects for each observation unit, given n observations, are accounted for. Here, 'Coefficients' refers to the factors within the model; 'dF/dx' denotes the partial derivatives displaying the marginal effects of the predictors (x'_{ik}) on y_i ('dbehavior'); 'SE' stands for Standard Error; 'z-value' denotes the test statistic obtained for each predictor; and 'Pr(>|z|)' refers to the associated p-value in a two-sided hypothesis test (where the null accounts for non-significance). The significance levels are: (*) significance at 10%; (**) significance at 5%; and (***) significance at 1%.

Fourth step: Confusion matrices

The first confusion matrix (Fig. 41) highlighted that whale sharks tended to assume an active surface ram – feeding behavior let the amount of chlorophylls increase, and that suction feeding actions can be associated with active surface ram – feeding ones (similar outcomes). Furthermore, an interesting result was that either active surface ram – feeding or suction feeding behavior took the highest probabilities when 'nchlorop' assumed value 2 (between 0.51-2,000 mg/m³ by construction). A possible explanation is that, in presence of massive chlorophylls

(value 3 by construction), the whale sharks would tend to change their behavior from active surface ram – feeding /suction feeding to ram (or passive) - feeding. This because it would require less effort by the whale sharks, but if and only if associated with favorable sea and weather conditions (according to PERMANOVA results). The predictive capability was 82.8%.

behaviors/chlorophylls	0	2	3
1 (A)	0.183	0.620	0.197
2 (P)	0.698	0.125	0.177
3 (V)	0.217	0.639	0.145

Figure 41 - Confusion matrix between feeding behaviors and chlorophylls. The values inside the table correspond to the joint probabilities between two discrete variables (Y and X) for each possible outcome. Here, Y refers to whale sharks' behavior and X refers to the number of chlorophylls grouped in classes. The sum of each row denoting the variable of interest gives one referring to probabilities.

The second confusion matrix (Fig. 42) between light levels and, consequently, water visibility (measured in oktas) and whale sharks' behavior, proved that better water visibility and then better water conditions (low oktas) would incline the whale sharks to assume active surface ram – feeding and suction feeding behaviors (very close results). However, when the oktas increased up to the maximum value (=8), ram (or passive) - feeding behavior increased, exceedingly so much active surface ram – feeding and suction feeding actions. Let the negative correlation matter between 'okta' and 'chlorop', the previous results and the findings found in TSMC and BSS held. The predictive capability was 84%.

behaviors/oktas	0	2	3	4	5	6	7	8
1 (A)	0.256	0.109	0.075	0.054	0.437	0.030	0.023	0.014
2 (P)	0.105	0.063	0.021	0.036	0.500	0.070	0.102	0.104
3 (V)	0.225	0.138	0.060	0.052	0.446	0.023	0.046	0.010

Figure 42 - Confusion matrix between feeding behaviors and water visibility. The values inside the table correspond to the joint probabilities between two discrete variables (Y and X) for each possible outcome. Here, Y refers to whale sharks' behavior and X refers water visibility measured through the predictor 'okta'. The sum of each row denoting the variable of interest gives one referring to probabilities.

In Figure 43, the confusion matrix between whale sharks' behavior and rainfall was displayed. With total absence of rain, active surface ram – feeding and suction feeding actions were

preferred dealing with better sea conditions and a sufficiently large presence of chlorophylls (negative relationship between ‘nrain’ and ‘nchlorop’). It highlighted the results found in the classification algorithms. The accuracy lined up on 88%.

behaviors/rainfall	0	2
1 (A)	0.998	0.003
2 (P)	0.928	0.072
3 (V)	0.967	0.33

Fig 43 - Confusion matrix between feeding behaviors and rainfall. The values inside the table correspond to the joint probabilities between two discrete variables (Y and X) for each possible outcome. Here, Y refers to WSs’ behavior and X refers to rainfall. The sum of each row denoting the variable of interest gives one referring to probabilities.

Concerning the surface water temperature, that optimal value would be $> 26\text{ C}^\circ$, where active surface ram – feeding and suction feeding actions are preferred (‘temperature’ close to 26.1 and 26.2 C° , respectively, just as found in BSS analysis). However, let the negative relationship matter between ‘ntemp’ and ‘nchlorop’, an increase in water temperature ($\geq 26.2\text{ C}^\circ$) would decrease the amount of chlorophylls, favouring ram (or passive) – feeding behavior and more suction feeding behavior than active surface ram – feeding one (Fig. 44). The predictive accuracy was 87.6%.

behaviors/surface water temperature	25.9	26.1	26.2
1 (A)	0.010	0.896	0.094
2 (P)	0.56	0.070	0.873
3 (V)	0.036	0.145	0.819

Figure 44 - Confusion matrix between feeding behaviors and surface water temperature. The values inside the table correspond to the joint probabilities between two discrete variables (Y and X) for each possible outcome. Here, Y refers to whale sharks’ behavior and X refers to water temperature. The sum of each row denoting the variable of interest gives one referring to probabilities.

Finally, evaluating the confusion matrix between whale sharks’ behavior and ENSO measurement unit in MEI (Fig. 45), whether this latter assumed values $\leq - 2.1$, active surface ram – feeding actions were preferred (just as found in BSS analysis). More precisely, restrained MEI would mean better sea and weather conditions, and then more chlorophylls. Conversely, an increase in MEI would tend to favor suction feeding actions and, in less quantity, ram (or

passive) - feeding behavior. Indeed, in the data, the maximum ENSO measurement unit was 1.3, generally associated with adequate sea and weather conditions. The predictive capability lined up on 88.4%.

behaviors/MEI	-1.2	-0.3	1.3
1 (A)	0.810	0.076	0.114
2 (P)	0.074	0.015	0.912
3 (V)	0.052	0.026	0.922

Figure 45 - Confusion matrix between feeding behaviors and ENSO measurement unit (MEI). The values inside the table correspond to the joint probabilities between two discrete variables (Y and X) for each possible outcome. Here, Y refers to whale sharks' behavior and X refers to El Niño measurement unit measured through MEI. The sum of each row denoting the variable of interest gives one referring to probabilities.

Let these findings mainly related to the strongly degree of dependency between whale sharks' behavior and amount of chlorophylls, a Cochran's Q test was performed to better emphasize it. Indeed, the hypothesis testing referred to independency (or causal choice, under the null) and dependency (or not causal choice, under the alternative). The test statistic was -179.51, and then it was sufficiently large to reject the null (p-value close to zero), confirming not only that whale sharks' behavior depended on the presence of chlorophylls but also on environmental factors. The significance level was 5% as default, with one degree of freedom.

Fifth step: Influence of the ENSO phenomenon on the interannual whale sharks' sightings in Djibouti

Let the Chi square test statistic be 243, with p-value close to zero, and 2 degrees of freedom (the degrees of freedom are computed as m-1, where m=3 denoting the number of time periods (2017, 2020, and 2022)), we can reject the null in favour of the alternative hypothesis. Thus, MEI, affecting weather conditions, would in turn be related to the number of sightings over time. However, since the data have been collected on three non-consecutive years only, a related confusion matrix was computed to analyse in depth that result. According to Figure 46, with predictive capability equals to 87.1%, the highest number of sightings has been recorded in 2022, with a MEI around -2.1, followed with lower sightings as MEI increased progressively (in 2020 with MEI = 1.3, and in 2017 with MEI = -0.3). It would highlight two main findings: (i) the number of sightings was positively affected with low MEI denoting adequate

water/weather conditions; and (ii) since ENSO measurement units collected in the data were very close between them, other factors such as water visibility, surface water temperature, rainfall, and concentration of chlorophylls had to be dealt with, just as achieved in the estimating procedure.

years/MEI	-1.2	-0.3	1.3
2017	0.000	1.000	0.000
2020	0.000	0.000	1.000
2022	1.000	0.000	0.000

Figure 46 - Confusion matrix between ENSO measurement unit (MEI) and total sightings. The values inside the table correspond to the joint probabilities between two discrete variables (Y and X) for each possible outcome. Here, Y refers to total sightings per year and X refers to ENSO measurement unit measured through MEI. The sum of each row denoting the variable of interest gives one referring to probabilities.

4. Discussion

4.1 Photoidentification

In November 2022, during the scientific expedition carried out by the Sharks Studies Center-Scientific Institute in Djibouti to study the ecology and ethology of whale sharks, 21 individuals were identified, and of 10 of them were catalogued as new individuals.

During the daily trips on the zodiacs there have been many resightings, where the same shark was sighted and recorded multiple times, both on the same day at different times and on different days. In order to detect and discard these individuals, the use of the I³S Classic has been essential. Despite not being internationally accepted as an identification method given the fact that it highly relies on an operator (Sacchi et al., 2016), it was of extremely importance to help the researchers identifying and discard those individuals seen multiple times and avoid mistaken analysis. Nonetheless, some individuals were not immediately marked as resightings by the program and have been added to the database as new individuals. Only after a careful examination by the researchers, based on the observation and comparison of the patterns of the sharks, it was possible to identify the individuals and mark them as resightings. The mistakes found both in the photoidentification and laser-photogrammetric analysis are driven by the difficulties to shot clear videos underwater. Water turbidity, air bubbles, other animals passing over the photoidentification area, a wide view of the camera, and reflected sunlight are all factors that can obscure and distort the pattern on the sharks useful for the identification (Steinmetz et al., 2018). For the photoidentification process, these factors can compromise the ability of the I³S Classic program to give a truthful match with the photos already present in the dataset. Concerning the laser photogrammetric survey also, if the two laser beams are not visible on the side of the shark, it is not possible to take a good frame and extrapolate the TL of the individual, or if the camera has distorted lens, the dimension of the animals are not respected, and the measure could be inaccurate.

In the year 2017 and 2020, 6 sharks have been identified respectively, for a total of 12 samples; in the year 2022, a total of 37 new sharks have been identified and added to the database. The increase in the sightings of sharks in Djibouti area during the years could be related to the increase in zooplankton biomass, that was just recorded from 2017 ($24.8 \pm 9.1 \text{ mg m}^{-3}$; Di Capua et al., 2021) to 2020 ($42.2 \pm 31.9 \text{ mg m}^{-3}$; Boldrocchi et al., 2020) in that area. Indeed, whale sharks exhibit temporal distribution associated with the variation in zooplankton biomass (Boldrocchi et al., 2020) and it is possible that a higher biomass of zooplankton drove them to aggregate in increasing numbers off the coasts of Djibouti over the years. However, a higher

number of whale sharks must be identified in the next years to confirm and make hypothesis about that.

After the identification of the new whale sharks in November 2022 and the completion of the identification sheets, most of them were recognized to be immature males, as in the other years also, presenting smooth claspers of short dimensions indicating that this population of whale sharks presents a demographic bias towards one sex and a specific maturity stage (Norman & Stevens, 2007). This is not an uncommon finding. Many studies reported that some aggregations are male dominated. For example, Araujo et al. (2019) stated that, in a group of 183 whale sharks collected and identified in the Philippines, 109 were males and 4 were females. In the Seychelles Islands, over a period of 8 years of data collection on whale sharks, 82% of the identified individuals were males and 18% were females while, over a period of 7 years of data collection in Djibouti, the identified males were 182 and the females 33 (Rowat et al., 2011). In southern Mozambique waters the sex bias was observed to be 75.7% for males and 24.3% for females (Rohner et al., 2015). The suggested explanation for this sex ratio in favour of immature males in Djibouti and in the other areas is that the sharks meet to feed and not for mating, given the low presence of both mature and immature females and mature males (Araujo et al., 2019).

On the other hand, there are other hotspots in the world that are dominated by immature females and pregnant females which inhabit deeper water offshore, like for example in the Galapagos Islands (Wingfield et al., 2018), and in the Gulf of California (Ramírez-Macías et al., 2012).

4.2 Laser-photogrammetric survey

The TLs obtained in Djibouti from the measured whale sharks were compared firstly to a study done in the same area which reported the average TL of the animals to be 3.7 m in 2012 (Rowat & Brooks, 2012); secondly, to the 12 identified and measured sharks during the Sharks Studies Centre expeditions in January 2017 and 2020 that presented an average TL of about 3 m in both years (an estimated value since laser-photogrammetry was not used); and lastly, to the 27 identified and measured sharks during the Sharks Studies Centre expedition in January 2022, where the average TL of the animals was reported to be 6.14 m.

The average TL of the sharks has increased of ± 2.35 m from 2012 to 2022, going from 3.7 m to 6.1 m on average, respectively.

The average TL of the new individuals measured in Djibouti in November 2022 (3 sharks) was 6.06 m, while the average TL of all the individuals measured in November was 6.05 m (Figure 33).

As we can see from the results, the average TLs of animals measured during the expeditions carried out in January and November 2022 differed by only 0.01 m. It is interesting like some of the sharks measured in January 2022 were also measured in November 2022 and the average TLs' differences between them was only of 0.22 m with the sharks of November being slightly shorter than the ones of January 2022. The difference in measurements between animals collected in different months of the same year (2022) could be related to the tools and the frames chosen for the analysis: by being slightly different frames and videos, the value calculated can be different. As we know from literature, whale sharks present slow growth rate (Colman, 1997), and being the expeditions carried out in 2022 only 10 months apart, the difference in size is perhaps minimal and hard to catch due to the difficulties to shot clear and consistent underwater videos.

Nonetheless, there was a great increase in TL of the identified sharks, passing from the average TL of 3.7 m in 2012 to the average TL of 6.06 m in 2022. This increase in size could be related again to the gradual increase in concentration of zooplankton biomass during the years (Boldrocchi et al., 2020; Di Capua et al., 2021) that induced a faster growth rate in TL of whale sharks and the exhibition of more suction feeding behaviors which, despite being energetically expensive, also allow a higher intake of food particles. The consequent energy gain could have permitted the growing of whale sharks, hence the difference in size between the years 2017 and 2022. Also in that case, more sharks must be measured in TL in the next years to make a similar hypothesis.

4.3 Influence of environmental factors on feeding behaviors and related annually ethograms

The statistical analysis about the influence of environmental factors on feeding behaviors showed that whale sharks exhibited differences in their feeding behaviors according to the variability of the environmental conditions (Fig. 37, and 38). Environmental factors resulted to be strictly correlated among them and their influence on feeding behaviors differed greatly (Fig. 37,38,40, OR results).

In particular, the feeding behaviors observed during all the expeditions carried out in Djibouti were analysed in relation to some environmental factors such as light levels, sea conditions, surface water temperature, rainfall, wind speed, time of the day, years of sampling collection, and ENSO phenomenon and chlorophylls concentration also. The latter was taken into consideration giving the positive correlation between chlorophylls concentration and zooplankton biomass (Gołdyn & Kowalczewska-Madura, 2008). Indeed, zooplankton is the main prey item of whale sharks, and it has a positive correlation with higher concentrations of

chlorophylls and, consequently, a higher biomass of phytoplankton on which zooplankton grazes on, increasing the presence of whale sharks.

Furthermore, the ENSO phenomenon was taken in consideration since different values of MEI were recorded during the years. Indeed, the ENSO is the most important coupled ocean-atmosphere phenomenon to cause global climate variability on seasonal to interannual time scales and it is known to affect marine ecosystems and marine animals' distribution, abundance, and behavior (Towner et al., 2013; Azevedo et al., 2022). The ENSO phenomenon is measured through the Multivariate ENSO Index (MEI). In particular, highest values of MEI represent the warm El Niño ENSO phase, while the lowest ones represent the cold La Niña ENSO phase (Towner et al., 2013). During warm El Niño events, the atmospheric pressure rises in the western Pacific Ocean and falls in the eastern Pacific Ocean, weakening or reversing the direction of southeast trade winds. This causes suppression of the thermocline (pushing it deeper), with a pool of warm water surging eastwards along the equator, towards South America and a reduction of the sea level in the western Pacific Ocean. On the contrary, the cold La Niña events lead to increased easterly winds and summer rainfall, reducing sea surface temperatures (Towner et al., 2013). ENSO events occur frequently each decade causing short to medium-term fluctuations in the climate and the periodicity of them varies between two and ten years with an average return period of three years. During these periods, anomalous physical conditions impact the marine biological systems (Towner et al., 2013).

The PERMANOVA test (Fig. 37) showed that all the environmental factors were significant at least at 10% and with the standard errors close to zero, so they were all able to influence the exhibition of feeding behaviors by whale sharks, and at the same time to predict them. The variables with the highest significance were oktas, surface water temperature, rainfall, and concentration of chlorophylls, as also reported by the OR results. The PERMANOVA test also showed that some variables were closely correlated: for example, chlorophylls concentration was negatively correlated with oktas and surface water temperature indicating that when the concentration of chlorophylls increases in the water, the underwater visibility is also high (less clouds present in the sky mean lower oktas values) and the surface water temperature is lower. Indeed phytoplankton, which contains chlorophylls, needs sunlight to live and grow (NOAA, 2023) and higher light levels increase the density of phytoplankton, and as a consequence of zooplankton, on which whale sharks feed mainly in active surface ram - feeding and suction feeding.

The negative correlation between chlorophylls concentration and surface water temperature, meaning that when the water was colder the concentration of chlorophylls was higher, could be explained by the seasonal upwelling in the northern Indian Ocean (Berumen et al., 2014).

Upwelling is the upward movement of seawater with a speed ranging from about 10^{-6} to 10^{-4} m/s, and colder water carrying from the lower layers to the upper ones, or the water surface is rich of nutrients and low in temperature favoring primary productivity (Hu & Wang, 2016). In the Indian Ocean, the upwelling events occur in the Northern hemisphere off Somalia, Oman, and India and, as they reach the coasts of Djibouti, these cold waters converge with the warm waters of the Red Sea creating an ideal environment for high biomass of chlorophylls, and consequently of phytoplankton and zooplankton (Boldrocchi et al., 2021). Hence the presence of *R. typus* and the observation of feeding behaviors such as active surface ram - feeding, and suction feeding occurred when there was a high and medium concentration of chlorophylls in the water (Fig. 38).

Another variable that affected the behavior of the whale sharks positively was sea conditions, which means that active surface ram - feeding, and suction feeding were preferred with rougher sea conditions. However, as it was seen in the PERMANOVA test (Fig. 37, and from the OR results), 'sea' had a low Pseudo-F indicating that probably the feeding behavior of the sharks was not strictly related to sea conditions but more to the concentration of chlorophylls in the water. In fact, rougher sea conditions increase the presence of chlorophylls by mixing the water column (Chen et al., 2020).

The logit function, the BSS results (Fig. 38, and Fig. 39, respectively) and the OR results highlighted that the concentration of chlorophylls was the most important variable in determining the feeding behavior of whale sharks, since it had the highest z-value and the highest significance in the logit function, the predictability of the active surface ram – feeding and suction feeding behaviors when values were higher than 0.60 mg/m^3 , and the highest OR result (75.18%). Chlorophylls concentration, however, as also seen in PERMANOVA test (Fig. 37), affected, and was affected, by all the other environmental parameters, since they were strictly related with them.

In fact, from the results of the logit function (Fig. 38), higher oktas, higher rainfall, and stronger winds, or in general worse weather conditions, would incline the whale sharks to assume a ram (or passive) - feeding behavior, mostly because the concentration of chlorophylls tends to decrease in these situations. The variable of rainfall predicted that with less rain the whale sharks were inclined to do active surface ram - feeding and suction feeding and, given the positive correlation between rainfall and concentration of chlorophylls, the latter increased when there was a low rainfall, favouring those behaviors. The fact that a little rainfall increases the concentration of chlorophylls in the water could be related to the increased amount of nutrients that are brought from land to the sea when the rain from the mainland reaches the water (Han et al., 2023). At the same time the surface water temperature decreases favoring

active surface ram - feeding and suction feeding (Witte et al., 2023). In fact, a strong negative correlation was also seen between concentration of chlorophylls and surface water temperature (Fig. 38): as the surface temperature of the water increases, the concentration of chlorophylls decreases, and the sharks are more inclined to choose a ram (or passive) - feeding behavior.

Figure 39 also showed the best set of variables that can correctly predict the behavior of the sharks, accordingly to what have been found in Figure 37, and 38. In fact, active surface ram - feeding and suction feeding were preferred when the surface water temperature was lower than 26.1°C, the concentration of chlorophylls was higher than 0.60 mg/m³, the rainfall was lower than 0.1 mm/h, and ENSO events were around -2.1 of MEI. Regarding the ENSO, with negative values representing La Niña events, surface water temperatures are colder, rainfall is lower in winter, and sky is clearer (Towner et al., 2013), all favourable situations making an increase of chlorophylls concentration helped also by roughest sea conditions that mix the surface water column.

The sample marginal effects depicted in Figure 39 showed and confirmed what found in PERMANOVA test and from OR results the concentration of chlorophylls, oktas, rainfall, surface water temperature, sea conditions, wind speed and time of the day were, in decreasing order, the environmental factors influencing the choice of the feeding behavior.

At this point the discussion we have answered at the first three questions: (i) the feeding behavior of whale sharks was affected by environmental factors strictly correlated between them; (ii) the variables that influenced the most the feeding behavior of the sharks were: concentration of chlorophylls, light levels, underwater visibility (measured through oktas), rainfall, and surface water temperature; (iii) the correlation between the environmental variables and climate change (ENSO) is proven by the fact that the latter has been omitted in the statistics (together with the variable years) because of its strongly correlation with more than one other variable.

The confusion matrices (Fig.41-45) confirmed what found in previous tests also. When the chlorophylls concentration was associated with high light levels' values (lower oktas values and, consequently, better underwater visibility) the sharks tended to assume active surface ram - feeding and suction feeding. However, when the concentration of chlorophylls was at the highest level associated with the highest oktas (cloudy sky) and worse underwater visibility, sharks tended to switch to ram (or passive) – feeding (as seen in Fig. 38). These results can be associated to the fact that each feeding mechanism requires different energy levels and ram (or passive) – feeding is the least expensive mechanism preferred when zooplankton presence is low and so the consequent energy gain is low also (Rohner & Prebble, 2021). However, with worse sea and weather conditions they preferred to use this feeding behavior instead of the more

energetic active and suction ones, even if the chlorophylls concentration was higher, trying to spend less energy.

Indeed, with the absence of rain, the sharks did active surface ram - feeding and suction feeding. On the contrary, when there was a low rainfall, a ram (or passive) - feeding behavior was preferred. These results agreed with the previous ones: in fact, when it does not rain, the sky can be clear or partially covered increasing underwater visibility and the concentration of chlorophylls inducing the sharks to favour active surface ram-feeding and suction feeding. On the other hand, if it rains, the okta levels are at the highest value and the sharks, in this case, prefer a ram (or passive)-feeding.

Furthermore, the relationship between surface water temperature and shark's feeding behavior showed that, when the temperature was colder and closer to 26°C, the sharks preferred suction and active surface ram-feedings which were also associated with higher concentration of chlorophylls, given the negative relationship between surface water temperature and concentration of chlorophylls. On the other hand, when the surface water temperature was warmer and closer to 26.2°C, the sharks showed a ram (or passive)-feeding behavior.

Finally, when the value of MEI was lower than -2.1, indicating La Niña ENSO events, the preferred behavior was active surface ram - feeding as it was found also in Figure 39. Moreover, a higher value of MEI, indicating El Niño ENSO events, favoured ram (or passive)-feeding and suction feedings.

The choice of the feeding behavior as a function of El Niño or La Niña ENSO events was related to the environmental factors influenced by this phenomenon. El Niño ENSO events (higher values of MEI) bring warmer surface water temperatures, cloudier sky and rainfall, and stronger wind speed (Towner et al., 2013) associated with ram (or passive) – feeding. On the other hand, La Niña ENSO events (lower values of MEI) bring colder surface water temperatures, clearer sky and low rainfall, and lower wind speed (Towner et al., 2013) associated with active surface ram – feeding and suction feeding.

Definitely, we can assess that:

Ram (or Passive) - feeding was observed mostly when:

1. Concentration of chlorophylls was lower.
2. Sky was cloudy (high values of oktas).
3. Rainfall was present.
4. Surface water temperature was higher.
5. El Niño ENSO events (or slightly La Niña ENSO events) occurred that sustained all the environmental conditions above.

All these factors and their values lead the attention to the fact that when the sharks exhibited ram (or passive)- feeding behavior, they did so for one main reason: to save energy. In fact, if the chlorophylls concentration is lower than a certain value, the sharks are seen in ram (or passive)- feeding because feeding actively is in general energetically expensive, and it is done only if the environmental conditions (that must be good) allow energy gain (Rohner & Prebble, 2021). Another variable related to energy consumption is the water temperature: at higher surface water temperatures the energy expense is higher; for example, white sharks (*Carcharodon carcharias*) also decreased the complexity and number of individual behaviors on the bait with higher temperatures to minimize the energy loss (Azevedo et al., 2022). It may be the case for whale sharks as well. In fact, ram (or passive)- feeding, where the hydrodynamic profile is not broken, allows for less expensive swimming, and it is observed when the surface water temperature is higher. Concerning the cloudiness of the sky, whale sharks present very small eyes compared to body size and they can use vision for prey identification just up to 100 m from the items (Yopak & Peele, 2021). In fact, sharks were seen performing ram (or passive)- feeding when the sky was cloudy and when it was raining, probably because the visibility decreased in the water and the sharks were not able to clearly see the prey.

Active surface ram - feeding and suction feeding were observed mostly when:

1. Concentration of chlorophyll was higher.
2. Sky was clear or partially covered (lower values of oktas).
3. Rainfall was absent.
4. Surface water temperature was close to 26°C.
5. La Niña ENSO events occurred that sustained all the environmental conditions above.

These results highlighted that active surface ram-feeding and suction feedings need similar environmental factors to be displayed. Again, concentration of chlorophylls was the most important variable predicting the feeding behavior of the sharks and, with less clouds in the sky and more visibility under the water, there was a higher concentration of chlorophylls due to higher sunlight, allowing the sharks to feed both actively and by suction. The surface water temperature was lower when they feed actively or in suction to minimize energy loss and maximize gain.

The frequency ethograms of the feeding behaviors showed great variations among the different years (2017, 2020, and 2022) and the results obtained were supported and explained by the environmental conditions recorded each year.

In 2017, the sharks preferred the ram (or passive) - feeding modality, followed by suction feeding, and active surface ram - feeding. Ram (or passive) - feeding behavior was preferred by the whale sharks possibly because the environmental factors were optimal for this choice of behavior. The chlorophylls concentration was reported to be 0.25 mg/m^3 , ranging in the lower margin of the range compared to the years 2020 (0.47 mg/m^3), and 2022 (0.50 mg/m^3 in January, and 2.0 mg/m^3 in November). The average light level value was of 5 oktas (partly covered sky, and worse underwater visibility), the rain was not present, the surface water temperature was of 26.1°C , MEI value was -0.3 meaning medium weather conditions close to El Niño ENSO event since the values were negative but close to 0, and the wind speed was low. All these data, with the only exception of the rain amount and wind speed, aligned with the prediction of ram (or passive) – feeding behavior. Given that chlorophylls concentration and light levels were the most important environmental factors according to OR results in influencing the choice of the behavior, their values in 2017 justified the exhibition of the ram (or passive) – feeding behavior. In addition, in the ethogram of 2017, sharks switched more frequently from active surface ram - feeding to suction feeding and vice versa . However, the environmental factors recorded highlighted that the concentration of chlorophylls in the water was low, but the oktas were not high (partly covered sky), there was no rain, and surface water temperature was balanced (these were the second, third, and fourth most important factors according to OR results), justifying this switching between active surface ram-feeding and suction feedings during the year.

In 2020, the analysis showed that suction feeding was the behavior most observed, followed by active surface ram - feeding and then ram (or passive) - feeding. The environmental factors reported for this year proved that the predictor influencing the choice of the feeding behavior was again the concentration of chlorophylls in the water. All the other variables did not show optimal values for this behavior. The chlorophylls concentration was reported to be 0.47 mg/m^3 , ranging in the medium range optimal for suction feeding; however, light levels were low (oktas were reported to be 7), the rainfall was present, the surface water temperature was measured to be 26.2°C , and the El Niño ENSO events was reported to be 1.3 indicating bad weather conditions. In this scenario we saw that the surface water temperature would predict the choose of the ram (or passive) - feeding instead of the suction feeding, and the El Niño ENSO value was 1.3, predicting the same behavior too. For that reason, in 2020, the only factor that could predict the choice of the suction feeding was the medium chlorophyll concentration. However, in 2020, sharks switched most frequently from suction feeding to ram (or passive) - feeding. In this case, the most observed behavior also corresponded to the one with higher

frequency in the ethogram and the other one, the ram (or passive) – feeding, responded to all the environmental factors occurred in 2020.

There were great differences in feeding behaviors exhibited also between the two 2022 expeditions, which were 10 months apart (January, and November). In January the most seen behavior was ram (or passive) - feeding, followed by suction feeding and active surface ram – feeding, whereas in November, the most seen was suction feeding, followed by ram (or passive) - feeding and closely by active surface ram - feeding. In January, the chlorophylls concentration was reported to be 0.56 mg/m^3 belonging in the medium range; light levels were very low (oktas were reported to be 8), no rainfall was recorded, the surface water temperature was 25.9°C , and La Niña ENSO value was of -2.1. All these variables, with the exception of the light levels' values, should affect the behavior of the sharks towards active surface ram - feeding and suction feeding. Despite the other variables, the most seen behavior was ram (or passive) - feeding probably because the value of oktas was very high (8), and from the statistical analysis in Figure 42 it was shown that when the value of oktas was of 8 and the sea conditions were good, the sharks preferred the ram (or passive) - feeding behavior.

During the expedition of November, on the other hand, the most observed behavior was suction feeding, and all the environmental factors were optimal for this behavior: the chlorophylls concentration was reported to be 1.9 mg/m^3 sitting in the highest range; light levels were good (oktas were reported to be 4), no rainfall was recorded, the surface water temperature was 25.9°C , and La Niña ENSO value was of -2.1. All these environmental factors predict that the sharks will tend to choose a suction feeding behavior, as they did.

In 2022 (January and November expeditions were analysed together being part of the same year), sharks switched from active surface ram - feeding to ram (or passive) - feeding and vice-versa. By analysing the factors recorded during the expeditions, we can conclude that the chlorophylls concentration was very high (November) or medium (January), and the oktas values were also high (January) or medium (November), and both these parameters are adequate for active surface ram feeding to switch to ram (or passive) – feeding and vice-versa.

Concluding, the feeding behavior of whale sharks were influenced by many factors, and in this study chlorophylls concentration was the most important one (as definitely confirmed also by the Cochran Q test) and it was related to the presence of whale sharks' preys, the zooplankton. A study located in the Bahia de Los Angeles in the eastern coast of Baja California Norte also suggested that the feeding behavior of whale sharks depends on the taxonomical abundance of prey present in the area that are consequently connected to the presence of phytoplankton and

chlorophylls in the water (Nelson & Eckert, 2007). Indeed, the active surface ram – feeding was exhibited with the highest concentration of prey and the highest taxonomic composition while, when sharks passed to suction feeding or ram (or passive) - feeding, both the concentration and the taxonomic composition of prey decreased (especially copepods densities) (Nelson & Eckert, 2007).

4.4 Influence of ENSO events on the interannual sightings of whale sharks in Djibouti

The statistical analysis showed that the ENSO measurement unit (MEI) was related to the number of sightings over the time only if considered strictly correlated with all the other environmental parameters (Chi square test, and Figure 46). In fact, by analysing the MEI, the highest number of sightings (37) were in 2022 with La Niña ENSO events, and with MEI values of -1.2, while in the years 2020 and 2017 we observed the same number of sightings (6, and 6 respectively) during El Niño ENSO events, with MEI values of 1.3 for 2020 and with a value close to El Niño ENSO event of -0.3 for 2017.

Higher number of whale sharks' sightings when the ENSO indicated years of La Niña events have been observed also by other studies in the Ningaloo Reef area (Australia). In particular, it has been observed that during El Niño ENSO years the sharks' sightings were lower compared with La Niña ENSO years (Wilson, 2001); the author suggested that it may be due to the fact that the changes in currents during the different El Niño/La Niña ENSO phases brought different amount of food resources available. Therefore, a weaker water currents during El Niño ENSO events would bring less food and consequently less sharks. On the contrary, in La Niña ENSO years, when the currents were stronger, a higher amount of food is brought to the area and more sharks were observed. This could have been happened also during the years of our study, but unfortunately the environmental factor of water currents has not been taken in consideration.

In addition, changes in water temperatures and prey availability induced by ENSO events can deeply influence the distribution and abundance of other ectothermic species such as the whale shark (Nakamura et al., 2020).

For example, the study of Arnés-Urgellés et al. (2021) on scalloped hammerhead sharks (*Sphyrna lewini*) showed that they feeding strategies adapted to the climate variability occurring during El Niño and La Niña ENSO events. In particular, during the warmer years of El Niño, it was suggested that the nutritional efficiency of scalloped hammerhead sharks decreased, and they became more generalist due to the warm waters and the absence of prey. On the contrary, during the cooler years of La Niña, with higher productivity and presence of prey, their foraging

activities increased, and sharks could feed on the preferred prey (Arnes-Urgelles et al., 2021). Moreover, another study highlighted that scalloped hammerhead sharks' numbers and abundance were greater during La Niña ENSO events and lower during El Niño ENSO events and the same pattern was observed also for tiger sharks (*Galeocerdo cuvier*) as they might have been responding to shifts in prey distributions (Osgood et al., 2020). These species showed the same abundance pattern of whale sharks. In contrast, *Mobula* rays exhibited little response to ENSO events, although this phenomenon is known to alter the distribution of zooplankton and larval fish prey (Osgood et al., 2020). The authors suggested that *Mobula* rays were a more resident species compared to the shark's species mentioned above (*S. lewini* and *G. curvier*) and that the site of the study was not of importance for the foraging ecology of *Mobula* rays, hence the reduced response to ENSO phenomenon (Osgood et al., 2020). Another species observed during the study of Osgood et al. (2020) was the whitetip reef shark (*Triaenodon obesus*) which, with its characteristic of being small and inactive, limits its need to shift the habitat in response to thermal changes. In fact, whitetip reef sharks showed the weakest response of all the examined species to ENSO phenomenon reflecting its lower metabolic rate (Osgood et al., 2021). Another study on blue sharks (*Prionace glauca*) found that the abundance of this species increased with strong La Niña events and that ENSO anomalies linked to warmer waters altered their distribution by altering the location of their prey favorable habitats (Adams et al., 2016).

During the expeditions of the Sharks Study Center - Scientific Institute carried out in Djibouti, 6 whale sharks were observed in 2017, when the value of MEI indicated -0.3 meaning weak La Niña events. In 2020, the number of sharks observed was also 6 and the MEI indicated 1.3 highlighting El Niño ENSO events. In 2022, the sharks added to the database were 37 and the MEI value was -2.1 indicating strong La Niña events. As it was observed, there were great differences in sightings of whale sharks in the years of strong La Niña compared to El Niño ENSO events. The years of La Niña ENSO events were characterized by higher chlorophylls concentration and cooler surface water temperatures, favoring both the presence of whale sharks which were attracted by the presence of zooplankton and more suitable surface water temperatures for active surface ram - feeding and suction feeding. On the contrary, the years of weak La Niña and El Niño ENSO events, when the primary productivity and the chlorophyll concentration were lower, did not show enough prey abundance to attract the whale sharks to feed in the area.

5. Conclusions

Photoidentification and laser-photogrammetry are two non-invasive techniques that can be used on many species to deepen demographic and migration studies and to manage conservation measures. *R. typus* is a species with optimal characteristics for both these techniques, especially due to its unique pattern, predictable presence, and gentle nature. One of the present thesis' goals was to contribute to increasing the number of whale sharks identified in the database of the Sharks Studies Center, which has been studying this species in Djibouti since 2017.

The new identified animals will help the Sharks Studies Center to deepen the knowledge on whale sharks' population, fundamental for their protection and conservation worldwide, specifically in Djibouti where they enrich the local population through ecotourism.

Also, the study of feeding behaviors and of how the environmental factors influence their exhibition and sharks' abundance and distribution in Djibouti area is fundamental, considering populations of whale sharks are declining globally.

It will be interesting in the future to compare the results of these expeditions in Djibouti to the others carried out in different areas, for example in Madagascar, with the aim to see in a fast-changing world if these animals and their feeding behaviors are affected by environmental factors and how they manage to survive.

Much research is still needed in many fields of *R. typus*. This giant fish undertakes long migrations which have not been fully understood and studied except for the aggregation's areas. New tools for tracking this species are needed, especially non-invasive satellite tags able to remain on the animals for long periods of time. Many studies have been conducted on immature males because sightings of adults, juvenile and pregnant females, and young smaller than 3 m are extremely rare. At the same time, nurseries have not been yet identified, probably because located in the abyss.

Ecotourism around whale sharks has increased exponentially in the last decade, and it is of primary importance to maintain these hotspots around the world and, at the same time, to respect and protect the sharks that aggregate there (Pierce et al., 2021). The aggregation spots of whale sharks are the only places, for now, where this species can be studied extensively and with minimal disturbance to the animals. The development of ecotourism has allowed for less expensive and overall easier research trips, but sensibilization of tourists and locals towards the respect of this giant of the oceans would help to preserve the feeding behaviors and migration patterns also to keep researching and exploring the mysteries of whale sharks.

Hoping that this thesis has contributed towards whale sharks' conservation and protection.



Scientific expedition in Djibouti, November 2022.
Lara Maule and the Sharks Studies Center Team

6. Appendix

- BORIS protocol
 1. Open BORIS -> folder: start_boris
 2. File -> new project ->
 - a. Information
 - b. Ethogram behavior
 - a= active surface ram-feeding
 - s= suction feeding
 - p= ram (or passive)-feedingstate event when the behavior has a start and a finish (point event when the behavior has not duration, es. jump)
select the key on the keyboard
 - p -> ram (or passive)-feeding
 - a -> active surface ram-feeding
 - s -> suction feedingmutually exclusive check all the squares because if an individual is in suction feeding, it is not ram (or passive) feeding.
 - c. Subject: all the animals names/sch in order of day/hour
Key: alphabetized in all caps b, c, d, e...
 - d. independent variables: they can be specified if they influence the behaviors (air temperature, water temperature, climatic conditions, aggregations, etc.)
 - e. Observation id: name of the video from the folder
 - f. Converters: if the data are exported from an outside source and are not expressed in seconds
 3. Observations -> new observation. New observation window will open
 - a. Obs ID: videos name from folder
 - b. Add media: select video from folder
 - c. Start
 - i. Subject key
 - ii. Start the video and start the coding
 - d. Save the project
 - e. New observation, edit the observation etc.
 4. Save each behavior class with time.
To export the data: observations -> export events -> aggregated events -> select all -> ok
In the section category select the wanted behavior -> ok
Save as: xlxs e give name -> save
 5. Extrapolate the transition matrices:
Observation -> create transition matrix -> frequencies of transitions -> Select all -> ok -> ok.
- 5. Create the ethogram
Tools ->transition flow diagram ->create transition flow diagram-> select the .tsv file (transition matrix from point 5) -> open-> ok
The flow diagram is now present in the transition matrix folder

7. References

- Adams, G., Flores, D., Flores, O., Aarestrup, K., & Svendsen, J. (2016). Spatial ecology of blue shark and shortfin mako in southern Peru: Local abundance, habitat preferences and implications for conservation. *Endangered Species Research*, 31, 19–32.
- Araujo, G., Agustines, A., Tracey, B., Snow, S., Labaja, J., et al. (2019). Photo-ID and telemetry highlight a global whale shark hotspot in Palawan, Philippines. *Scientific Reports*, 9(1), Article 1.
- Arnés-Urgellés, C., Salinas-de-León, P., Rastoin-Laplane, E., Vaca-Pita, L., Suárez-Moncada, J., et al. (2021). The Effects of Climatic Variability on the Feeding Ecology of the Scalloped Hammerhead Shark (*Sphyrna lewini*) in the Tropical Eastern Pacific. *Frontiers in Marine Science*, 8, 625748.
- Arzoumanian, Z., Holmberg, J., & Norman, B. (2005). An astronomical pattern-matching algorithm for computer-aided identification of whale sharks *Rhincodon typus*. *Journal of Applied Ecology*, 42(6), 999–1011.
- Azevedo, O. M., Correia, A. M., Micarelli, P., Reinero, F. R., Rijllo, G., et al. (2022). Sex Differences in the Individual Behaviour of Bait-Attracted White Sharks (*Carcharodon carcharias*, Linnaeus, 1758) Are Linked to Different Environmental Factors in South Africa. *Biology*, 11(12), Article 12.
- Baldrige, H. D. (1970). Sinking Factors and Average Densities of Florida Sharks as Functions of Liver Buoyancy. *Copeia*, 1970(4), 744–754.
- Bava, P., Micarelli, P., & Buttino, I. (2022). Zooplankton assemblage diversity in the whale shark *Rhincodon typus* aggregation area of Nosy Be (Madagascar). *Estuarine, Coastal and Shelf Science*, 279, 108159.
- Bean, B.A. (1907). The history of the whale shark (*Rhinodon typicus* Smith). *Smithsonian Miscellaneous Collections*, 48: 144.
- Becerril-García, E. E., Pancaldi, F., Cruz-Villacorta, A. A., Rivera-Camacho, A. R., Aguilar-Cruz, C. A., et al. (2021). General descriptions of the dermis structure of a juvenile whale shark *Rhincodon typus* from the Gulf of California. *Journal of Fish Biology*, 99(4), 1524–1528.
- Berumen, M. L., Braun, C. D., Cochran, J. E. M., Skomal, G. B., & Thorrold, S. R. (2014). Movement Patterns of Juvenile Whale Sharks Tagged at an Aggregation Site in the Red Sea. *PLOS ONE*, 9(7), e103536.
- Boldrocchi, G., Omar, M., Azzola, A., & Bettinetti, R. (2020). The ecology of the whale shark in Djibouti. *Aquatic Ecology*, 54(2), 535–551.
- Boldrocchi, G., Schmidt, J. V., & Robinson, D. P. (2021). First documented record of the leatherback turtle (*Dermochelys coriacea*) from Djibouti waters. *Marine Biodiversity Records*, 14(1), 3.
- Borrell, A., Aguilar, A., Gazo, M., Kumarran, R. P., & Cardona, L. (2011). Stable isotope profiles in whale shark (*Rhincodon typus*) suggest segregation and dissimilarities in the diet depending on sex and size. *Environmental Biology of Fishes*, 92(4), 559–567.

- Casper, B. M., & Mann, D. A. (2009). Field hearing measurements of the Atlantic sharpnose shark *Rhizoprionodon terraenovae*. *Journal of fish biology*, 75(10), 2768-2776.
- Chen, C. T., Liu, K. M., & Joung, S. J. (2002). Preliminary report on Taiwan's whale shark fishery. In *Elasmobranch Biodiversity, Conservation and Management: Proceedings of the International Seminar and Workshop, Sabah, Malaysia, July 1997* (pp. 162-167).
- Chen, M., Pattiaratchi, C. B., Ghadouani, A., & Hanson, C. (2020). Influence of Storm Events on Chlorophyll Distribution Along the Oligotrophic Continental Shelf Off South-Western Australia. *Frontiers in Marine Science*, 7.
- CITES (2003) Checklist of CITES Species: A Reference to the Appendices to the Convention on International Trade in Endangered Species of Wild Fauna and Flora. *UNEP World Conservation Monitoring Centre*, Cambridge, UK
- Colman, J. G. (1997). A review of the biology and ecology of the whale shark. *Journal of Fish Biology*, 51(6), 1219–1234.
- Compagno, L.J.V. (1984). An annotated and illustrated catalogue of shark species known to date. Part 1—Hexanchiformes to Lamniformes. *FAO Species Catalogue*. Vol. 4, Sharks of the world. *FAO Fisheries Synopsis*, 125: 209–211.
- Dean, M. N., & Summers, A. P. (2006). Mineralized cartilage in the skeleton of chondrichthyan fishes. *Zoology*, 109(2), 164–168.
- Di Capua, I., Micarelli, P., Tempesti, J., Reinerio, F.R., & Buttino, I. (2021). Zooplankton size structure in the Gulf of Tadjoura (Djibouti) during whale shark sighting: a preliminary study. *Cahiers de Biologie Marine*, 62(3): 290-294.
- Dove, A.D., Meekan, M.G., & McClain, C.R. (2021). How and Why Is the Whale Shark the World's Largest Fish? *Whale Sharks: Biology, Ecology, and Conservation*, 1:1-12.
- Dove, A.D.M. (2015). Foraging and ingestive behaviors of whale sharks, *Rhincodon typus*, in response to chemical stimulus cues. *Biological Bulletin*, 228: 65-74.
- Fay, R.R. & Popper, A.N. (1980). Structure and function in teleost auditory systems. *Comparative studies of hearing in vertebrates*. *Springer-Verlag New York*. 1980: 3-42.
- Fox, S., De La Parra-Venegas, R., Galván-Pastoriza, B.E., Graham, R.T., Hoffmayer, E. R., et al. (2013) Population structure and residency of whale sharks *Rhincodon typus* at Utila, Bay Islands, Honduras. *Journal of Fish Biology*, 83(3): 574-587.
- Friard, O. & Gamba, M. (2016). BORIS: a free, versatile open-source event-logging software for video/audio coding and live observations. *Methods in Ecology and Evolution*, 7: 1325–1330.
- Gardiner, J.M., Atema, J., Hueter, R.E., & Motta, J.P. (2014). Multisensory integration and behavioral plasticity in sharks from different ecological niches. *PLoS One*, 9(4): e93036.
- Gleiss, A.C., Norman, B., & Wilson, R.P. (2011). Moved by that sinking feeling: variable diving geometry underlies movement strategies in whale sharks. *Functional Ecology*, 25(3): 595-607.
- Gołdyn, R., & Kowalczyńska-Madura, K. (2008). Interactions between phytoplankton and zooplankton in the hypertrophic Swarzędzkie Lake in western Poland. *Journal of Plankton Research*, 30(1), 33–42.

- Hamlett, W.C. (1999), *Sharks, Skates and Rays: the biology of elasmobranch fishes*. Johns Hopkins University Press. *Princeton and Oxford*, 31-33.
- Han, H., Xiao, R., Gao, G., Yin, B., Liang, S., et al. (2023). Influence of a heavy rainfall event on nutrients and phytoplankton dynamics in a well-mixed semi-enclosed bay. *Journal of Hydrology*, 617, 128932.
- Hara, Y., Yamaguchi, K., Onimaru, K., Kadota, M., Koyanagi, M., et al. (2018). Shark genomes provide insights into elasmobranch evolution and the origin of vertebrates. *Nature Ecology & Evolution*, 2(11), Article 11.
- Hart, N., Lisney, T., & Collin, S. (2006). Visual communication in elasmobranchs (pp. 338–392).
- Hu, J., & Wang, X. H. (2016). Progress on upwelling studies in the China seas. *Reviews of Geophysics*, 54(3), 653-673.
- Hueter, R.E., Tyminski, J.P., & De la Parra, R. (2013). Horizontal movements, migration patterns, and population structure of whale sharks in the Gulf of Mexico and northwestern Caribbean Sea. *PLoS One*, 8(8): e71883.
- Kardong, V. & Kennet, V. (2002), *Vertebrates. Comparative anatomy, function, evolution*. Third edition. *Mc Graw-Hill*, 96-101.
- Legaspi, C., Miranda, J., Labaja, J., Snow, S., Ponzo, A., et al. (2020). In-water observations highlight the effects of provisioning on whale shark behaviour at the world's largest whale shark tourism destination. *Royal Society Open Science*, 7(12): 200392.
- Leigh, S.C., Papastamatiou, Y., & German, D.P. (2017). The nutritional physiology of sharks. *Reviews in Fish Biology and Fisheries*, 27: 561-585.
- Marshall, A.D. & Pierce, S.J. (2012). The use and abuse of photographic identification in sharks and rays. *Journal of Fish Biology*, 80(5): 1361–1379.
- Marsili, L., Consales, G., Romano, P., Rosai, R., Bava, P., et al. (2023). A Cocktail of Plankton and Organochlorines for Whale Shark in the Foraging Areas of Nosy Be (Madagascar). *Diversity*, 15(8), 911.
- Martin, R.A. (2007). A review of behavioural ecology of whale sharks (*Rhincodon typus*). *Fisheries Research*, 84(1), 10-16.
- Martino, C., Morton, J. T., Marotz, C. A., Thompson, L. R., Tripathi, A., et al. (2019). A Novel Sparse Compositional Technique Reveals Microbial Perturbations. *MSystems*, 4(1), 10.1128/mSystems.00016-19
- McClain, C.R., Balk, M., A., Benfield, M.C., Branch, A.T., & Chen, C., et al. (2015). Sizing ocean giants: patterns of intraspecific size variation in marine megafauna. *PeerJ*, 3: e715.
- Micarelli, P., Buttino, I., Bava, P., Cappelletti, G., Andrani, N., Massa, M., Marsella, A., Vernelli, E., & Reinerio, F. R. (n.d.). Photoidentification as a complementary tool to evaluate whale shark movements between different areas: The case of Nosy Be in Madagascar and the Gulf of Tadjoura in Djibouti.
- Motta, P.J. & Wilga C.A.D. (1995). Anatomy of the feeding apparatus of the lemon shark, *Negaprion brevirostris*. *Journal of Morphology*, 226(3): 309-329.

- Motta, P.J., Maslanka, M., Hueter, R.E., Davis, R.L., De la Parra, R., et al. (2010). Feeding anatomy, filter-feeding rate, and diet of whale sharks *Rhincodon typus* during surface ram filter feeding off the Yucatan Peninsula, Mexico. *Zoology*, 113(4): 199-212.
- Muller, M. (1999). Size limitations in semicircular duct systems. *Journal of Theoretical Biology*, 198(3): 405-437.
- Nakamura, I., Matsumoto, R., & Sato, K. (2020). Body temperature stability in the whale shark, the world's largest fish. *Journal of Experimental Biology*, 223(11), jeb210286.
- Nelson, J. & Eckert, S. (2007), Foraging ecology by whale sharks (*Rhincodon typus*) within Bahía de Los Angeles, Baja California Norte, Mexico. *Fisheries Research*, 84: 47–64.
- Norman, B. (2005). The whale shark. *MESA Information Sheet, Marine Education Society of Australasia. CITES Identification Manual Whale Shark*. (n.d.).
- Norman, B., M. & Stevens, J., D., (2007). Size and maturity status of the whale shark (*Rhincodon typus*) at Ningaloo Reef in Western Australia. *Fisheries Research* 84.1: 81-86.
- Norman, B.M., & Morgan, D.L. (2016). The return of “Stumpy” the whale shark: two decades and counting. *Frontiers in Ecology and the Environment*, 14: 449-50.
- Pierce, S.J. & Norman, B. (2016). *Rhincodon typus*. The IUCN Red List of Threatened Species, 2016.
- Pierce, S.J., Grace, M.K., & Araujo, G. (2021). *Rhincodon typus* (Green Status assessment). The IUCN Red List of Threatened Species, 2021.
- Pierce, S.J., Pardo, S.A., Rohner, C.A., Matsumoto, R., Murakumo, K., et al. (2021). 2 Chapter: Whale Shark Reproduction, Growth, and Demography. *Whale Sharks: Biology, Ecology, and Conservation*, 1: 13-46.
- Pillans, R. (2003). *Nebrius ferrugineus*. The IUCN Red List of Threatened Species, 2003.
- Ramírez-Macías, D., Vázquez-Haikin, A., & Vázquez-Juárez, R. (2012). Whale shark *Rhincodon typus* populations along the west coast of the Gulf of California and implications for management. *Endangered Species Research*, 18(2), 115-128.
- Reynolds, S.D., Norman, B.M., Franklin, C.E., Bach, S.S., Comezzi, F.G. et al. (2022). Regional variation in anthropogenic threats to Indian Ocean whale sharks. *Global Ecology and Conservation*, 33: e01961.
- Robinson, D.P., Jaidah, Y.M., Bach., S.S., Rohner, C.A., Jabado, W.R., et al. (2017). Some like it hot: repeat migration and residency of whale sharks within an extreme natural environment. *PLoS One*, 12(9): e0185360.
- Rohner, C. A., & Prebble, C. E. (2021). Whale Shark Foraging, Feeding, and Diet. *Whale Sharks: Biology, Ecology, and Conservation*, 1: 153-180.
- Rohner, C.A., Armstrong, A.J., Pierce, S.J., Prebble, C.E.M., Cagua, E.F., et al. (2015). Whale sharks target dense prey patches of sergestid shrimp off Tanzania. *Journal of Plankton Research*, 37: 352–362.

- Rowat, D. & Brooks, K.S. (2012). A review of the biology, fisheries, and conservation of the whale shark *Rhincodon typus*. *Journal of Fish Biology*, 80(5): 1019–1056.
- Rowat, D., Brooks, K., March, A., McCarten, C., Jouannet, D., et al. (2011). Long-term membership of whale sharks (*Rhincodon typus*) in coastal aggregations in Seychelles and Djibouti. *Marine and Freshwater Research*, 62(6), 621-627.
- Sacchi, R., Scali, S., Mangiacotti, M., Sannolo, M., & Zuffi, M. A. (2016). Digital identification and analysis. Reptile ecology and conservation. *A handbook of techniques*, 59-72.
- Shadwick, R.E., & Goldbogen, J.A. (2012). Muscle function and swimming in sharks. *Journal of Fish Biology*, 80(5): 1904-1939.
- Sherwood, L., Klandorf, H., & Yancey P. (2012). Animal physiology: from genes to organisms. *Cengage Learning*, 1: 401-403.
- Smith, A. (1828). Descriptions of new, or imperfectly known objects of the animal kingdom, found in the south of Africa. *South African Commercial Advertiser*, 3: 2.
- Speed, C.W., Meekan, M.G., & Bradshaw, C.J.A. (2007) Spot the match—wildlife photo-identification using information theory. *Frontiers in Zoology*, 4: 2.
- Steinmetz, K., Webster, I., Rowat, D., & Bluemel, J. K. (2018). Evaluating the software I3S Pattern for photo-identification of nesting hawksbill turtles (*Eretmochelys imbricata*). *Marine Turtle Newsletter*, 155, 15-19.
- Taylor, G. (2007). Ram filter-feeding and nocturnal feeding of whale sharks (*Rhincodon typus*) at Ningaloo Reef, Western Australia. *Fisheries Research*, 84: 65–70.
- TIES, 2003. What is Ecotourism? *The International Ecotourism Society*.
- Tomita, T., Murakumo, K., Komoto, S., Dove, A., Kino, M., et al. (2020) Armored eyes of the whale shark. *PLoS One*, 15(6): e0235342.
- Towner, A. V., Underhill, L. G., Jewell, O. J. D., & Smale, M. J. (2013). Environmental Influences on the Abundance and Sexual Composition of White Sharks *Carcharodon carcharias* in Gansbaai, South Africa. *PLoS ONE*, 8(8), e71197
- Tuma, R. E. (1976). An investigation of the feeding habits of the bull shark, *Carcharhinus leucas*, in the Lake Nicaragua-Rio San Juan system. *Investigations of the ichthyofauna of Nicaraguan lakes*. 1: 533-539
- Tyminski, J.P., De la Parra-Venegas, R., Gonzales-Cano, J., & Hueter, E.R. (2015). Vertical movements and patterns in diving behavior of whale sharks as revealed by pop-up satellite tags in the eastern Gulf of Mexico. *PloS One*, 10(11): e0142156.
- Van Tienhoven, A.M., Den Hartog, J.E., Reijns, R., & Peddemors, V.M. (2007) A computer-aided program for pattern-matching of natural marks of the spotted ragged tooth shark *Carcharias taurus* (Rafinesque, 1810). *Journal of Applied Ecology*, 44: 273–280.
- Wilson, S. G., Taylor, J. G., & Pearce, A. F. (2001). The seasonal aggregation of whale sharks at Ningaloo Reef, Western Australia: currents, migrations and the El Niño/Southern Oscillation. *Environmental Biology of Fishes*, 61: 1-11.

- Wingfield, J. C., Hau, M., Boersma, P. D., Romero, L. M., Hillgarth, N., et al. (2018). Effects of El Niño and La Niña Southern Oscillation events on the adrenocortical responses to stress in birds of the Galapagos Islands. *General and comparative endocrinology*, 259: 20-33.
- Wintner, S.P. (2000). Preliminary study of vertebral growth rings in the whale shark, *Rhincodon typus*, from the east coast of South Africa. *Environmental Biology of Fishes*, 59: 441–451.
- Witte, C. R., Zappa, C. J., & Edson, J. B. (2023). The Response of Ocean Skin Temperature to Rain: Observations and Implications for Parameterization of Rain-Induced Fluxes. *Journal of Geophysical Research: Oceans*, 128(1), e2022JC019146.
- Womersley, F.C., Humphries, N.E., Queiroz, N., & Sims, D.W. (2021). Global collision-risk hotspots of marine traffic and the world’s largest fish, the whale shark. *Proceedings of the National Academy of Sciences*, 119(20): e2117440119.
- Yopak, K.E. & Peele, E.E. (2021). Whale Shark Sensory Biology and Neuroanatomy. *Whale Sharks: Biology, Ecology and Conservation*, 1: 47-64.
- Ziegler, J.P.D. & Dearden, P. (2021). Whale shark tourism as an incentive-based conservation approach. *Whale sharks: Biology, ecology, and conservation*, 1: 109.

Photos bibliography

- Figure 2: Dove, A.D., Meekan, M.G. & McClain, C.R. (2021). How and Why Is the Whale Shark the World’s Largest Fish? *Whale Sharks: Biology, Ecology, and Conservation*, 1: 1-12.
- Figure 13: Rohner, C.A. & Prebble, C.E. (2021). Whale Shark Foraging, Feeding, and Diet. *Whale Sharks: Biology, Ecology, and Conservation*, 1: 153-180.
- Figure 3: Denison, R. (1937) Anatomy of the head and pelvic fin of the whale shark, *Rhincodon typus*. *Bulletin of the AMNH*, 73: 5.
- Figure 1, 6a, 17, 18, 19, 29, 30, 31, 32, 33: photo by Lara Maule, Djibouti 2022.
- Figure 8: Norman, B.M., & Stevens, J.D. (2007). Size and maturity status of the whale shark (*Rhincodon typus*) at Ningaloo Reef in Western Australia. *Fisheries Research*, 84(1): 81-86.
- Figure 9, 11: Yopak, K.E. & Peele, E.E. (2021). Whale Shark Sensory Biology and Neuroanatomy. *Whale Sharks: Biology, Ecology and Conservation*, 1: 47-64.
- Figure 12: photo by Pietro Storelli, Djibouti 2022.
- Figure 14: Tomita, T., Murakumo, K., Komoto, S., Dove, A., Kino, M., et al. (2020) Armored eyes of the whale shark. *PLoS One*, 15(6): e0235342.
- Figure 26: photo by Sibilla Dolci, Djibouti 2022.
- Figure 25, 26, 27, 28, 34: photo by Centro Studi Squali (Sharks Studies Centre).
- Figure 24: photo by Enrico Vittorini, Djibouti 2022.

Sitography

- <https://www.copernicus.eu/en>
- <https://www.windguru.cz/4910>
- <https://www.isprambiente.gov.it>
- <https://psl.noaa.gov/enso/mei.old/mei.html>
- <https://oceanservice.noaa.gov/facts/phyto.html>

Photos sitography

- Figure 4,7, 15: <https://wetpixel.com/>
- Figure 5, 6b: <https://www.floridamuseum.ufl.edu/discover-fish/species-profiles/rhincodontypus/>.
- Figure 10: <https://cdna.artstation.com/>
- Figure 16: left: <https://a-z-animals.com/blog/what-do-zooplankton-eat/>, right: <https://www.algaebarn.com/blog/copepods/a-primer-on-the-different-characteristics-and-uses-of-the-major-copepod-groups/>
- Figure 20, 21: <https://www.iucnredlist.org/species/19488/2365291>
- Figure 22: <https://www.redsea-project.com/>
- Figure 23: www.mapsofworld.com